

FINAL REPORT

Global Radiative Effect of Particulate Black Carbon

by

Serena H. Chung

The Cooperative Institute for Research in Environmental Sciences

NOAA Aeronomy Laboratory

Boulder, CO 80503

and

John H. Seinfeld

Departments of Chemical Engineering and Environmental Science and Engineering

California Institute of Technology

Pasadena, CA 91125

Contract #02-322

Principal Investigator:

John H. Seinfeld, California Institute of Technology

Prepared for the California Air Resources Board and the California Environmental
Protection Agency

May 2, 2005

Disclaimer

The statements and conclusions in this Report are those of the contractor and not necessarily those of the California Air Resources Board. The mention of commercial products, their source, or their use in connection with material reported herein is not to be construed as actual or implied endorsement of such products.

Acknowledgments

This Report was submitted in fulfillment of ARB contract number 02-322 titled Global Radiative Effect of Particulate Black Carbon by California Institute of Technology under the sponsorship of the California Air Resources Board. Work was completed as of January 25, 2005.

Contents

Disclaimer	i
Acknowledgments	ii
List of Figures	iv
List of Tables	v
Abstract	vi
Executive Summary	vii
1 Introduction	1
2 Model Description	5
3 Results	24
4 Discussion	37
5 Summary and Conclusions	38
6 Recommendations	39
References	41

List of Figures

1	Estimated global emissions of aerosol components and gaseous aerosol precursors.	12
2	Wavelength-dependent optical properties for aerosols in the dry state.	16
3	Estimates of global burden for (a) carbonaceous and (b) inorganic aerosols.	25
4	Estimates of global mean direct radiative forcings at TOA (top panel) and at the surface (bottom panel) and for individual aerosol (left panel) and aerosol mixtures (right panel).	29
5	Predicted geographical distributions of predicted anthropogenic contribution to annual mean TOA direct radiative forcing (W m^{-2}) for the year 2100 for (a) Externally-mixed BC, (b) Internally-mixed BC, (c) POA, and (d) $\text{SO}_4^{2-}/\text{NH}_4^+/\text{NO}_3^-/\text{H}_2\text{O}$. The global averages are given on the upper right hand corner of each figure.	30
6	Predicted geographical distributions of predicted anthropogenic contribution to annual mean direct radiative forcing at the surface (W m^{-2}) for the year 2100 for (a) Externally-mixed BC, (b) Internally-mixed BC, (c) POA, and (d) $\text{SO}_4^{2-}/\text{NH}_4^+/\text{NO}_3^-/\text{H}_2\text{O}$. The global averages are given on the upper right corner of each figure.	31
7	Predicted indirect radiative forcing of anthropogenic sulfate aerosol.	32
8	Geographical distribution of predicted indirect radiative forcing of anthropogenic sulfate aerosol for the year 2025.	34

List of Tables

ES-1	Estimates of Anthropogenic Direct Radiative Forcing at TOA (W m^{-2})	xiv
ES-2	Estimates of Anthropogenic Direct Radiative Forcing at the Surface (W m^{-2})	xv
ES-3	Predicted Indirect Radiative Forcing of Anthropogenic Sulfate Aerosol (W m^{-2})	xvi
1	Summary of Inorganic Aerosol Model	5
2	Summary of Chemical Reactions for Modeling Inorganic Aerosols	8
3	Summary of Carbonaceous Aerosol Model	9
4	Summary of Estimated Global Emissions of Aerosol Components and Gaseous Aerosol Precursors	11
5	Aerosol Physical and Optical Properties at $\lambda=550$ nm in the Dry State.	15
6	Predicted Global Aerosol Burdens (Tg)	25
7	Estimates of Anthropogenic Direct Radiative Forcing at TOA (W m^{-2})	27
8	Estimates of Anthropogenic Direct Radiative Forcing at the Surface (W m^{-2})	28
9	Predicted Indirect Radiative Forcing of Anthropogenic Sulfate Aerosol (W m^{-2})	33

Abstract

The primary objective of this research was to provide the ARB with state-of-the-science global radiative forcing estimates for black carbon and other aerosols in conjunction/comparison with other greenhouse gases. These estimates, both at top of the atmosphere and at the surface, were obtained over 25-year intervals for 2000, 2025, 2050, 2075, 2100, based on Intergovernmental Panel on Climate Change (IPCC) estimates of emissions over the next century.

Carbon dioxide (CO₂) and other greenhouse gases and black carbon (BC) particulate matter influence global climate. With reference to potential measures to abate the effect of California emissions of greenhouse gases and particulate matter on climate, it is necessary to determine the current magnitude of that effect relative to the estimated full global impact. The present report focuses on global climatic effects of BC, and, based on an estimate of the percentage of global BC emissions attributable to California, extrapolates that effect to California emissions alone. Since black carbon particulate matter tends to mix with other particulate material in the atmosphere, the radiative effect of BC needs to be considered in conjunction with that of other aerosol species, namely, sulfate, nitrate, ammonium, and primary organic aerosol; the manner in which BC is mixed with other particulate species is quite important to its radiative impact. In the current study, we have estimated present-day BC emissions from California by scaling the recent BC inventory of *Bond et al.* [2004] to California on the basis of population. Based on population, California is estimated to contribute approximately 0.4% of the global mean direct radiative forcing attributable to anthropogenic BC aerosol. Assuming that BC is mixed with other aerosol species, the contribution of California emissions to top of atmosphere direct radiative forcing is currently estimated to be +0.002 W m⁻², predicted to increase to +0.008 W m⁻² in 2100.

Executive Summary

Background

Assembly Bill 1493 requires the Air Resources Board to develop and adopt regulations that achieve the maximum feasible reduction of greenhouse gases emitted by passenger vehicles and light-duty trucks and other noncommercial vehicles. The goal of this Bill is to place California among the forefront of states in adopting measures to alleviate “global warming”. While CO₂ is the predominant greenhouse gas, black carbon particles also exert a climatic warming influence; an important question is the relative radiative forcing potentials of CO₂ and black carbon aerosols. Motor vehicles emit a significant amount of fine organic carbon and black carbon (BC) particles. Recent studies suggest a significant climatic effect of BC particles, released in part from diesel and gasoline engines. Black carbon particles exert a warming effect in the atmosphere similar to that of greenhouse gases but, in contrast, cool the surface of the earth. Their heat-trapping ability depends on the extent to which they are co-mixed with other substances in more chemically complex particles. Quantitative understanding of the absorbing aerosols role in climate forcing is required to accurately evaluate the radiative forcing impacts of PM emissions versus those of greenhouse gases.

The primary objective of this research was to provide the ARB with state-of-the-science global radiative forcing estimates for black carbon and other aerosols in conjunction/comparison with other greenhouse gases. These estimates, both at top of the atmosphere and at the surface, were obtained over 25-year intervals for 2000, 2025, 2050, 2075, 2100, based on Intergovernmental Panel on Climate Change (IPCC) estimates of emissions over the next century.

Anthropogenic-induced changes in the atmospheric abundance of greenhouse gases and particulate matter are estimated to make significant contributions to climate change over the next century [IPCC, 2001]. Important anthropogenic particulate species include sulfate (and associated inorganic ions) and carbonaceous compounds. The particles alter the radiative balance of Earth’s surface and atmosphere by two types for forcings: direct and indirect. Direct radiative forcing is the change in the net radiative flux (in W m⁻²) due to the scattering or absorption of radiation by aerosols. The amount of light scattered and absorbed depends on the optical properties, which are governed by the refractive indices, size, and shape of the aerosols. Particles can also change the microphysics of cloud formation by acting as cloud condensation nuclei (CCN). Changes in cloud properties, such as albedo and lifetime, also alter the radiative flux of the atmosphere, and this change is defined as indirect radiative forcing.

Carbon in particulate matter can take a variety of forms. Typically, these are divided into three main components: organic carbon (OC), a refractory component also known as elemental carbon (EC), and carbonate carbon (CO₃²⁻). For the purposes of global radiative forcing emissions inventories, BC is defined as the carbon component

of particulate matter that absorbs light. For estimates of global radiative forcing, BC is generally considered as equivalent to EC. The principal source of black carbon is combustion. Except for natural fires, whose sources are small on a global basis, most black carbon derives from either biomass burning or fossil fuel combustion.

Both organic and black carbon affect the extinction of solar radiation. Black carbon is the principal light-absorbing aerosol species (some dust particles and condensed aromatic hydrocarbons may also contribute to light absorption), while both organic and black carbon aerosols are light-scattering species. Carbonate carbon is a constituent of mineral dust. From a climatic point of view, organic carbon acts similarly to sulfate in that it largely scatters solar radiation and cools the Earth-atmosphere system by reflecting some portion of the incoming sunlight back to space that would otherwise reach the surface. In contrast to sulfate and organic carbon, black carbon is a strong absorber of solar radiation. By absorbing radiation in the atmosphere and preventing that radiation from reaching the Earth's surface, black carbon has the opposite effects of warming the atmosphere but cooling the surface.

As mentioned previously, particulate matter also affects the climate by means of indirect forcing. The problem of estimating the indirect forcing of atmospheric aerosols is very complex as many parameters, such as aerosol size distribution and chemical composition, may be influential. An additional limitation is the cloud parameterizations in global models. Cloud formation is a complicated process which includes updraft velocities, entrainment and detrainment and other subgrid-scale processes that are difficult to accurately represent in global models with low spatial resolution. The IPCC [2001] does not state a best estimate for the indirect forcing of anthropogenic aerosols, but gives an uncertainty range between 0 to -4.8 W m^{-2} .

Methods

Direct radiative forcings of black carbon, primary organic aerosol, and inorganic system of $\text{SO}_4^{2-}/\text{NH}_4^+/\text{NO}_3^-/\text{H}_2\text{O}$ aerosol and indirect radiative forcings of sulfate aerosol are estimated for the years 2000, 2025, 2050, 2075, and 2100. First, the global distribution for each type of aerosol is simulated for the preindustrial period and for the years 2000, 2025, 2050, 2075, and 2100 online in a three-dimensional climate model. Then radiative forcing is calculated at top of the atmosphere and at the surface for each time period. The climate model used is the the NASA Goddard Institute for Space Studies General Circulation Model II-prime. Direct radiative forcing calculation is based on the optical properties of the aerosols, assumed size distributions, and Mie-scattering theory. Indirect radiative forcing calculation of sulfate aerosol is based on empirical correlations. The anthropogenic contribution to radiative forcing is determined by subtracting the preindustrial forcing from the total forcing.

Three-dimensional global transport of aerosols and relevant gas-phase species is simulated on-line in the Goddard Institute for Space Studies General Circulation Model II-prime (GISS GCM II-prime), which is described by *Hansen et al.* [1983].

Since the present study was initiated, GISS has completed development of the next generation version of the GCM II', which is referred to as the GISS model E [*Schmidt et al.*, 2005], which has been adopted as the new standard GISS model with the present version designated as model III. Model E is a reprogrammed, modularized and documented version of prior GISS climate models including improved representations of several physical processes. *Schmidt et al.* [2005] compare simulations with $2^\circ \times 2.5^\circ$ and $4^\circ \times 5^\circ$ horizontal resolutions, finding that the climatology of the $4^\circ \times 5^\circ$ version is almost as realistic as the finer resolution in most respects.

On-line simulation predicts the concentrations of H_2O_2 , dimethyl sulfide (DMS), methanesulfonic acid (MSA), SO_2 , NH_3 , SO_4^{2-} , NO_3^- , NH_4^+ and aerosol water. Gas-phase reactions of DMS with OH and NO_3 radicals and oxidation of SO_2 by OH are included, as well as aqueous oxidation of SO_2 by H_2O_2 inside clouds. Monthly average three-dimensional concentration fields for NO_3 radicals are imported in the GISS GCM from the work of *Wang et al.* [1998] and five-day-average three-dimensional concentration fields for OH and OH_2 are imported from the work of *Spivakovsky et al.* [2000]. The concentrations are assumed to be constant for all time periods. For the purpose of determining aerosol nitrate concentrations, total nitric acid concentration fields are taken from the the Harvard-GISS GCM for the preindustrial period, 2000, and 2100 [*Mickley et al.*, 1999]. For the years 2025, and 2050, and 2075, nitric acid concentrations are interpolated linearly between the 2000 and 2100 results.

Aerosol dynamics and composition are treated with a simple bulk model (no aerosol size distribution) of internally mixed SO_4^{2-} , NO_3^- , NH_4^+ , and H_2O . This mixture is assumed to be in thermodynamic equilibrium with the gas phase. Equilibrium concentrations are calculated using the gas-particle inorganic equilibrium model ISORROPIA [*Nenes et al.*, 1998] at every dynamical time step. All chemical components of inorganic aerosol are considered to be infinitely soluble in clouds for the purpose of computing wet deposition.

Simulation of carbonaceous aerosols follows the methodology of *Chung and Seinfeld* [2002]. Carbonaceous aerosols included in the model are black carbon (BC) and primary organic aerosol (POA). POA are organic particles that are emitted directly into the atmosphere from fossil fuel, biofuel, and biomass burning. For the purpose of representing wet scavenging, each of these two classes of aerosol is divided into hydrophobic and hydrophilic categories, for a total of four tracers for carbonaceous aerosols.

Organic aerosol can also form in the atmosphere from gas-to-particle conversion of oxidation products of volatile organic compounds (VOCs). This category of OC is called secondary organic aerosol (SOA). SOA formation has increased globally since preindustrial times due to the increase in POA, which provide the absorptive medium into which the semi-volatile oxidation products can condense. SOA is excluded from this study because its contribution to the global OC burden is relatively small [*Chung and Seinfeld*, 2002]. Also, among the VOCs, only hydrocarbons of biogenic origin are found to contribute significantly to global SOA formation. Therefore, SOAs are inherently natural, even though their concentrations increase indirectly as a result of

anthropogenic activities.

Country-specific inventories of climate change are compiled under the United Nations Framework Convention on Climate Change [UNFCCC, 2001]. Currently, over 180 countries subscribe to the agreement, although not all have produced climate change inventories. Climate change emissions inventories prepared under the UNFCCC generally conform with guidelines developed by the Intergovernmental Panel on Climate Change (IPCC). These inventories typically focus on the greenhouse gases (CO_2 , CH_4 , N_2O , HFC, PFC, and SF_6); however, most also include volatile organic compounds (VOC), nitrogen oxides (NO_x), and carbon monoxide (CO) and many include other pollutants such as sulfur dioxide (SO_2). To date, the national climate change inventories do not include BC, OC, or particulate matter. The global BC emissions inventory of *Bond et al.* [2004] is employed in the present study.

To project how global aerosol radiative forcing might change as the current century progresses, six different time periods have been simulated: preindustrial (roughly corresponding to the year 1800), modern day (year 2000), and the years 2025, 2050, 2075, and 2100. For future emission rates, emission scenario A2 of the IPCC Special Report on Emission Scenarios (SRES) [Nakicenovic and Swart, 2000] is used. Anthropogenic sulfur emissions for the modern day and the future are prescribed based on the IPCC SRES A2 emission scenario. Preindustrial sulfur emissions include only DMS from the oceans and volcanic SO_2 emissions. Since atmospheric DMS is biogenic in origin, DMS emissions are assumed to be the same for all time periods. Volcanic emissions of SO_2 are also assumed to be constant. Ammonia emissions are based on the Global Emissions Inventory Activity (GEIA) [Bowman et al., 1997], which provides estimated emissions for the year 1990. For the year 2000, annual emissions of black carbon and primary organic aerosols are taken from the emission inventory of *Bond et al.* [2004], with estimated present-day global BC emission rates being 1.6, 3.3, and 3.0 Tg yr^{-1} for biofuel, open burning, and fossil fuel, respectively. *Bond et al.* [2004] provide only annual emissions; the biomass burning inventory is distributed monthly by scaling the annual emissions by monthly fire counts of the Global Burned Area 2000 Project [Grégoire et al., 2003]. Fossil fuel and biofuel emissions are assumed to be constant throughout the year.

The mixing state of black carbon with other aerosols is important in determining its radiative effect [Chýlek et al., 1995; Haywood et al., 1997; Myhre et al., 1998; Jacobson, 2000]. To bound the impact of aerosol mixing state on direct radiative forcing, two limiting cases are considered. In one case, each aerosol component (sulfate, organic carbon, black carbon) is assumed to be contained in physically separate particles, forming an external mixture. In the other case, each particle consists of a homogeneous mixture of all species present, i.e. the aerosols are internally mixed.

Several types of aerosol indirect effects have been identified, either observationally or in theory, based on the various mechanisms through which aerosols perturb cloud albedo. Twomey [1977] and Twomey et al. [1984] identified the first indirect effect in which increased cloud condensation nucleus (CCN) concentrations result in increased

cloud droplet concentrations, smaller drop radii, and more reflective clouds. The Twomey effect, which is the only indirect effect considered by the IPCC [2001], assumes there are no aerosol-induced changes in cloud liquid water content or cloud fraction. Relaxing this assumption allows a number of secondary indirect effects in which cloud albedo is changed through changes in liquid water content or cloud fraction [Albrecht, 1989; Boers and Mitchell, 1994; Pincus and Baker, 1994]. Our understanding of the indirect effects can be represented through models that simulate aerosol-cloud-climate interactions on scales ranging from cloud parcel models (meters) to cloud resolving models (kilometers) and ultimately to GCMs (global).

The specific aspect of indirect climate forcing of aerosols that is of interest here is to estimate the indirect forcing attributable to black carbon aerosols. When initially emitted into the atmosphere, black carbon particles are assumed in most current studies to be hydrophobic. By definition, hydrophobic particles will not act as cloud condensation nuclei and therefore do not contribute to aerosol indirect forcing. It is generally assumed that black carbon particles become coated with hydrophilic material as they age in the atmosphere through condensation of gases, principally sulfuric acid and volatile organics. Once black carbon becomes coated with a soluble material, the resulting composite particle may act as a CCN; only in this way may black carbon play a role in indirect forcing.

The approach that is still most widely used to model indirect aerosol forcing on a global scale is to employ empirical relationships between cloud droplet number concentration and aerosol sulfate mass [IPCC, 2001]. Using this approach, sulfate aerosols are implicitly assumed to control indirect aerosol forcing. If black carbon happens to be present in the sulfate particles as a result of atmospheric processing, that black carbon acts simply as an insoluble inclusion in the particle. Since sulfate is highly water-soluble and most sulfate particles are generally large enough to act as CCN, the effect of the insoluble inclusion on the CCN behavior of the particles is insignificant.

Hansen *et al.* [2005] have investigated the efficacies of the first and second aerosol indirect effects, AIE₁ and AIE₂, via parameterizations that are included as options in GISS GCM Model III. The parameterization is based on observed empirical effects of aerosols on cloud droplet number concentration (N_d) [Menon and Del Genio, 2004]. They include four time-variable aerosols: sulfate (S), nitrate (N), black carbon (BC), and organic carbon (OC), with the distributions and histories of each of these based on simulations of Koch *et al.* [1999] and Koch [2001].

Results

Direct radiative forcing of black carbon is predicted to warm the climate while that of primary organic aerosol and sulfate aerosol is predicted to cool the climate. Direct radiative forcings of anthropogenic black carbon and primary organic aerosol are linearly proportional to their emission rates and are predicted to increase continuously from 2000 to 2100, whereas, based on IPCC SRES emissions scenario A2, direct

radiative forcing of $\text{SO}_4^{2-}/\text{NH}_4^+/\text{NO}_3^-/\text{H}_2\text{O}$ aerosol increases from 2000 to 2050, and then levels off from 2050 to 2100 because SO_2 emissions are predicted to decrease after 2050. For the same reason, indirect radiative forcing of sulfate follows the same trend as direct radiative forcing of $\text{SO}_4^{2-}/\text{NH}_4^+/\text{NO}_3^-/\text{H}_2\text{O}$ aerosol.

Of all particulate species, black carbon exerts the most complex effect on climate. Like all aerosols, BC scatters a portion of the direct solar beam back to space, which leads to a reduction in solar radiation reaching the surface of the Earth. This reduction is manifest as an increase in solar radiation reflected back to space at the top of the atmosphere, that is, a *negative* radiative forcing (cooling). A portion of the incoming solar radiation is absorbed by BC-containing particles in the air. This absorption leads to a further reduction in solar radiation reaching the surface. At the surface, the result of this absorption is cooling because solar radiation that would otherwise reach the surface is prevented from doing so. However, the absorption of radiation by BC-containing particles leads to a heating in the atmosphere itself. Thus, absorption by BC leads to a negative radiative forcing at the surface and a positive radiative forcing in the atmosphere. Finally, the BC-containing aerosol absorbs radiation from the diffuse upward beam of scattered radiation. This reduces the solar radiation that is reflected back to space, leading to a positive radiative forcing at the top of the atmosphere. This effect is particularly accentuated when BC aerosol lies above clouds.

Top-of-atmosphere (TOA) forcing for BC is the sum of the negative forcing at the surface due to scattering of incoming radiation and the positive forcing from absorption of upward diffuse radiation. The absorption of incoming solar radiation by BC does not contribute to TOA forcing because it adds heat to the atmosphere but reduces solar heating at the surface by the same amount. The net effect of BC is to add heat to the atmosphere and decrease radiative heating of the surface. The TOA radiative forcing for BC is the sum of the surface (negative) and atmospheric (positive) forcing.

Estimates of global mean direct forcing are summarized in Tables ES-1 and ES-2. For internally mixed aerosols, identifying the contribution of each component to the total radiative forcing is difficult because total radiative forcing is not a just sum of those due to individual components. For the purpose of estimating the maximum BC contribution to direct radiative forcing, we take the direct radiative forcing of BC in an internal mixture to be the difference in radiative forcing between that of the internal mixture of BC, POA, and $\text{SO}_4^{2-}/\text{NH}_4^+/\text{NO}_3^-/\text{H}_2\text{O}$ aerosols and that of an external mixture of POA and $\text{SO}_4^{2-}/\text{NH}_4^+/\text{NO}_3^-/\text{H}_2\text{O}$ aerosols. The magnitude of both TOA and surface forcing for each individual species scales linearly with predicted global burden. Under the external mixture assumption, the forcing efficiencies at TOA are approximately $+2.8 \text{ W m}^{-2}$ per Tg of anthropogenic BC, -0.18 W m^{-2} per Tg of anthropogenic POA, and -0.12 W m^{-2} per Tg of anthropogenic $\text{SO}_4^{2-}/\text{NH}_4^+/\text{NO}_3^-/\text{H}_2\text{O}$ aerosol, in agreement with forcing efficiencies determined by *Chung and Seinfeld* [2002]. At the surface, the forcing efficiencies are -4.5 W m^{-2} per Tg of anthropogenic BC, -0.17 W m^{-2} per Tg of anthropogenic POA, and -0.11 W m^{-2} per Tg of anthropogenic $\text{SO}_4^{2-}/\text{NH}_4^+/\text{NO}_3^-/\text{H}_2\text{O}$ aerosol.

m^{-2} per Tg of anthropogenic $\text{SO}_4^{2-}/\text{NH}_4^+/\text{NO}_3^-/\text{H}_2\text{O}$ aerosol. When internally mixed with other aerosols, the forcing efficiencies of BC increase to +5.4 and -6.4 at TOA and the surface, respectively.

While cooling of $\text{SO}_4^{2-}/\text{NH}_4^+/\text{NO}_3^-/\text{H}_2\text{O}$ aerosol is predicted to level off after 2050 as SO_2 emission decreases, warming by BC and cooling by POA are predicted to increase. For BC, anthropogenic direct radiative forcing at TOA is estimated to increase from +0.4 to +1.1 W m^{-2} from year 2000 to 2100 if BC is externally mixed with other aerosols. If BC is internally mixed with POA and $\text{SO}_4^{2-}/\text{NH}_4^+/\text{NO}_3^-/\text{H}_2\text{O}$ aerosol, then the increase is from +0.7 to +2.1 W m^{-2} . Compared to BC, the magnitude of direct radiative forcing of anthropogenic POA is relatively small.

Under the external mixture assumption, by the year 2100, the combined effect of BC, POA, and $\text{SO}_4^{2-}/\text{NH}_4^+/\text{NO}_3^-/\text{H}_2\text{O}$ aerosols is that the net cooling at TOA is almost the same as the present day ($\sim 0.5 \text{ W m}^{-2}$); however, because of increased absorption of solar radiation by BC in the atmosphere, the cooling at the surface is more than doubled from -1.5 to -3.6 W m^{-2} . Under the internal mixture assumption, the effect of BC is even greater. In this case, the net effect of direct radiative forcing of anthropogenic BC, POA, and $\text{SO}_4^{2-}/\text{NH}_4^+/\text{NO}_3^-/\text{H}_2\text{O}$ at TOA is changed from net cooling of 0.1 W m^{-2} in 2000 to net warming of 0.5 W m^{-2} by 2100. Clearly, by 2100, based on the SRES A2 emissions scenario direct radiative forcing of BC is predicted to be as important as that of $\text{SO}_4^{2-}/\text{NH}_4^+/\text{NO}_3^-/\text{H}_2\text{O}$ aerosol.

Estimates of global mean indirect forcing attributable to sulfate aerosols are summarized in Table ES-3. As expected, indirect radiative forcing leads to net cooling at TOA as increased sulfate concentrations leads to increased cloud albedo, reflecting more solar radiation back to space. Note that the magnitude of the surface forcing is slightly greater than that at TOA because multiple reflections within the atmospheric column prevent even more solar radiation from reaching the surface. Indirect radiative forcing is predicted to be largest in the year 2025 as 2025 is the year of the greatest SO_2 emission.

The efficacy of a climate forcing can be defined as the global mean temperature change produced by the forcing relative to the global mean temperature change produced by a CO_2 forcing of the same magnitude. Hansen introduced this effective forcing concept and terminology because it was realized that the climate effect of pollutants such as soot and ozone was complex, depending especially on their spatial distribution. CO_2 provides an apt basis for comparison, because the anthropogenic increase of atmospheric CO_2 is the largest anthropogenic climate forcing [IPCC, 2001]. Attempts to slow global warming must focus primarily on restricting CO_2 emissions. Therefore, in considering the merits of reducing other forcings, it is helpful to know their contributions to global warming relative to that of CO_2 . Efficacies are computed based on a 100 year simulation (or longer) and therefore include all climate feedbacks that operate on that time scale.

Absorbing aerosols, like BC, represent the prime climate forcing agent for which the magnitude of radiative forcing is not necessarily a good indicator of the climate response, that is, the efficacy can be much different from unity. Hansen et al. [2005]

Table ES-1: Estimates of Anthropogenic Direct Radiative Forcing at TOA (W m^{-2})

Aerosol	Year				
	2000	2025	2050	2075	2100
<i>Individual Component</i>					
BC	+0.39	+0.54	+0.68	+0.85	+1.15
POA	-0.10	-0.14	-0.17	-0.21	-0.28
$\text{SO}_4^{2-}/\text{NH}_4^+/\text{NO}_3^-/\text{H}_2\text{O}$	-0.74	-1.31	-1.40	-1.25	-1.37
<i>Mixture</i>					
External	-0.44	-0.90	-0.89	-0.60	-0.49
Internal	-0.10	-0.41	-0.25	+0.17	+0.49
<i>BC contribution to Internal Mixture^a</i>					
	+0.75	+1.03	+1.31	+1.62	+2.13

^a BC contribution to forcing of the internal mixture is calculated as forcing of the internal mixture minus that of an external mixture of POA and $\text{SO}_4^{2-}/\text{NH}_4^+/\text{NO}_3^-/\text{H}_2\text{O}$.

Estimated present-day greenhouse gas radiative forcings [*IPCC*, 2001]:

CO_2 :	+1.46	CH_4 :	+0.48
N_2O :	+0.15	Halocarbons:	+0.34
Total:	+2.43		

find that BC aerosols from biomass burning have a calculated efficacy of 59%, while fossil fuel BC has an efficacy of 79%. Predicted global warming is close to 1°C when all the BC is assumed to be in the planetary boundary layer and 0.3°C when the BC is all in the free troposphere. Thus the climate efficacy of BC decreases markedly as more of the BC is found in the upper troposphere. The large change in efficacy with the altitude of BC is due, in part, to the reduction in cloud cover that results from heating of the layer by BC. Heating of the layer containing the aerosols lowers cloud cover in that layer, but that heating also inhibits convection from the layer below and, in so doing, leads to an increase in cloud cover in the layer below. *Roberts and Jones* [2004] studied the climate sensitivity to fossil fuel black carbon using the Hadley Centre GCM. They obtained a climate sensitivity of 0.56°C per W m^{-2} for BC versus 0.91°C per W m^{-2} for CO_2 . Thus, their fossil fuel BC efficacy is about 62%, as compared with the 79% obtained by *Hansen et al.* [2005]. Because BC climate efficacy is so sensitive to the altitude distribution of BC, more work will be

Table ES-2: Estimates of Anthropogenic Direct Radiative Forcing at the Surface (W m^{-2})

Aerosol	Year				
	2000	2025	2050	2075	2100
<i>Individual Component</i>					
BC	-0.63	-0.87	-1.09	-1.36	-1.82
POA	-0.15	-0.20	-0.26	-0.32	-0.43
$\text{SO}_4^{2-}/\text{NH}_4^+/\text{NO}_3^-/\text{H}_2\text{O}$	-0.70	-1.25	-1.34	-1.20	-1.31
<i>Mixture</i>					
External	-1.48	-2.32	-2.70	-2.88	-3.56
Internal	-1.74	-2.67	-3.14	-3.42	-4.24
<i>BC contribution to Internal Mixture^a</i>					
	-0.89	-1.22	-1.54	-1.90	2.50

^a BC contribution to forcing of the internal mixture is calculated as forcing of the internal mixture minus that of and external mixture of POA and $\text{SO}_4^{2-}/\text{NH}_4^+/\text{NO}_3^-/\text{H}_2\text{O}$.

needed to better constrain these efficacies.

Of critical interest to the present study is to associate the portions of the indirect aerosol effect with each aerosol type. Because of the complexity of aerosols, with internal and external mixtures of various compositions and the idealized representations of aerosols in climate models, it is not possible at present to accurately apportion the indirect effect. Nevertheless, *Hansen et al.* [2005] make an idealized apportionment of the indirect effect among aerosol types. Their computation includes sulfates, nitrates, black carbon and organic carbon as aerosols. They carry out climate simulations, in which they remove individually the indirect effect of each of the four time-variable aerosols. This was done by retaining the direct effect of all aerosols, but excluding a specific aerosol from calculation of the aerosol indirect effect on clouds. The results of such a run were then subtracted from the results of the run that included the full direct and indirect effects of all aerosols. Only the effect of aerosols on cloud cover was considered, but its forcing (-1.01 W m^{-2}) was such as to approximate the estimate for the total aerosol indirect effect.

Hansen et al. [2005] conclude that with the external mixing assumption the aerosol indirect effect is apportioned as sulfates (36%), organic carbon (36%), nitrates (22%), black carbon (6%). But they caution that this estimate, the first of its type, is highly uncertain.

Table ES-3: Predicted Indirect Radiative Forcing of Anthropogenic Sulfate Aerosol (W m^{-2})

	2000	2025	2050	2075	2100
TOA	-0.96	-1.25	-1.25	-0.99	-0.92
Surface	-1.04	-1.34	-1.34	-1.06	-0.99

The small contribution of black carbon to aerosol indirect forcing computed by Hansen et al. is consistent with an assessment based on aerosol mixing state and the role of BC-containing particles acting as cloud condensation nuclei. *Therefore, for the purposes of the present study, we conclude that indirect aerosol forcing by black carbon is essentially negligible. Stated differently, the level of indirect aerosol forcing by black carbon is of a sufficiently small magnitude that it lies well within the uncertainty bounds of a number of the more important input parameters, such as emissions and atmospheric mixing state.*

According to Bond et al. [2004], BC emissions from contained combustion (i.e. fossil fuel and biofuel combustion) in North America is currently 382 Gg yr^{-1} . The total population in North America is 428 million, of which about 35 million live in California. Using population as a proxy, then current BC emissions from California due to contained combustion are approximately 31 Gg yr^{-1} , which is approximately 0.4% of the present-day estimated global emission of anthropogenic BC. Assuming that radiative forcing scales linearly with emission rate, then the State of California is responsible currently for approximately 0.4% of the global mean direct radiative forcing attributable to BC. Under the external mixture assumption, fossil fuel and biofuel BC currently emitted in California is predicted to contribute to TOA direct radiative forcing an amount equal to $+0.001 \text{ W m}^{-2}$, with this forcing increasing to $+0.005 \text{ W m}^{-2}$ by 2100. If BC is internally mixed with POA and $\text{SO}_4^{2-}/\text{NH}_4^+/\text{NO}_3^-/\text{H}_2\text{O}$, then the contribution from California increases to $+0.002$ and $+0.008 \text{ W m}^{-2}$ for 2000 and 2100, respectively.

Conclusions

As global SO_2 emissions slowly decline according to IPCC SRES emissions scenario A2, anthropogenic black carbon is predicted to become an increasingly important contributor to total direct radiative forcing toward the end of the current century. The effect of black carbon is especially significant if black carbon is internally mixed with primary organic aerosol and $\text{SO}_4^{2-}/\text{NH}_4^+/\text{NO}_3^-/\text{H}_2\text{O}$ aerosol. By 2075, a net

global warming is predicted for the internal mixture of black carbon, primary organic aerosol, and $\text{SO}_4^{2-}/\text{NH}_4^+/\text{NO}_3^-/\text{H}_2\text{O}$. Even when cooling by indirect radiative forcing of sulfate is considered, warming due to internally-mixed BC can potentially cancel out the combined cooling due to other aerosols. Based on population, California is estimated to contribute approximately 0.4% of the global mean direct radiative forcing of anthropogenic BC.

The motivation of the present study is to obtain an estimate of the climatic effect of black carbon emissions from the State of California. Given such an estimate, one can then proceed to compare the relative climatic effects of CO_2 and black carbon emitted by California. This will provide state legislators with information needed when considering CO_2 and BC abatement policies motivated by future climate effects.

As in all studies of global climate effects of gases and aerosols, the most important input is the emissions themselves. In the current study, we have estimated present-day BC emissions from California by scaling the recent BC inventory of *Bond et al.* [2004] to California on the basis of population. The extent to which this estimate is accurate is unknown. Therefore, our first recommendation is that the State of California prepare a current emissions inventory for black carbon particulate matter (We understand that this is already underway.) Because of the role of BC particulate matter in both climate and human health effects, this endeavor is highly recommended.

A next step in this overall project is to study climatic effects on California of greenhouse gas and aerosol radiative forcing over the next century. This would involve evaluating different greenhouse gas and aerosol emission scenarios, with special attention to the relative emissions of CO_2 and black carbon. Climatic effects would include surface temperature and precipitation rates and patterns. Such a study would require a GCM having as fine a spatial resolution as possible, so as to be able to resolve climatic variations on a spatial scale of California. The results of the current study can serve as input information to such a climate study.

In this report we have argued that indirect climatic effects of BC on cloud formation are small owing to the fact that BC must become coated by soluble aerosol material before being able to function as a CCN, and that, on a mass basis, soluble sulfate and organic carbon substantially exceed that of BC globally. This argument is supported by the very recent work of *Hansen et al.* [2005], which estimates that about 6% of global indirect aerosol forcing can be attributed to BC. Nevertheless, current estimates of indirect forcing, on the whole, remain quite uncertain; even more uncertain are the contributions to indirect aerosol forcing by individual aerosol species. Such contributions are even more difficult to unravel because aerosols in the atmosphere generally exist as internal mixtures. Research continues to be carried out actively worldwide aimed at trying to understand and unravel indirect aerosol effects. Still, the extent to which aerosol indirect forcing (by sulfates and organic aerosols predominantly) will affect the hydrological cycle in California should be examined using the best current aerosol/cloud parameterizations available for GCMs.

1 Introduction

Anthropogenic-induced changes in the atmospheric abundance of greenhouse gases and particulate matter are estimated to make significant contributions to climate change over the next century [*Intergovernmental Panel on Climate Change (IPCC)*, 2001]. Radiative forcing and climate impact of greenhouse gases have been studied extensively in the literature (see e.g. Chapter 9 of IPCC [2001]). These studies point to emission control of greenhouse gases as a method of curtailing global warming. Many papers also address the climate forcing of anthropogenic aerosols [*Charlson et al.*, 1991; *Kiehl and Briegleb*, 1993; *Taylor and Penner*, 1994; *Boucher and Anderson*, 1995; *Chuang et al.*, 1997; *Feichter et al.*, 1997; *Haywood et al.*, 1997; *Penner et al.*, 1997, 1998; *Koch et al.*, 1999; *Kiehl et al.*, 2000; *Tegen et al.*, 2000; *Adams et al.*, 2001; *Ghan et al.*, 2001; *Koch*, 2001; *Jacobson*, 2000; *Chung and Seinfeld*, 2002], but most of them emphasize only present-day emission scenarios. Quantitative understanding of the aerosol's role in climate forcing due to increased emissions in future scenarios is required to accurately assess the radiative forcing impacts of anthropogenic particle emission versus those of greenhouse gases.

Important anthropogenic particulate species include sulfate (and associated inorganic ions) and carbonaceous compounds. The particles alter the radiative balance of Earth's surface and atmosphere by two types of forcings: direct and indirect. Direct radiative forcing is the change in the net radiative flux (in W m^{-2}) due to the scattering or absorption of radiation by aerosols. The amount of light scattered and absorbed depends on the optical properties, which are governed by the refractive indices, size, and shape of the aerosols. Particles can also change the microphysics of cloud formation by acting as cloud condensation nuclei (CCN). Changes in cloud properties, such as albedo and lifetime, also alter the radiative flux of the atmosphere, and this change is defined as indirect radiative forcing.

The first-order estimate of the climate impact of an atmospheric constituent is the radiative forcing it induces, which measures the net change in incoming and outgoing irradiance, usually calculated at top of the atmosphere (TOA) or at the tropopause. The concept of radiative forcing as a measure of climate change is justified by the assumption that, for small perturbations, the equilibrium global and annual mean surface air temperature change ($\Delta[\bar{T}_s]$) is approximately linearly related to the global and annual mean radiative forcing ($\Delta[\bar{F}]$), i.e.

$$\Delta[\bar{T}_s] = \lambda\Delta[\bar{F}], \tag{1}$$

where λ is the climate sensitivity in units of $\text{K W}^{-1} \text{ m}^2$. Indeed, climate model experiments have shown that, for relatively spatially homogeneous radiative forcing, λ is reasonably independent of the nature of the forcing within an individual climate model (within 20%). For example, *Hansen et al.* [1984,1997], *Forster et al.* [2000], and *Joshi et al.* [2003], show that the climate responses for doubled CO_2 and a 2% increase in solar irradiance are remarkably similar even though solar forcing affects shortwave radiation and CO_2 mainly affects longwave radiation.

An important factor in the linear relationship of Equation (1) is that $\Delta[\bar{F}]$ needs to be defined appropriately. The IPCC Assessment [IPCC, 2001] defines radiative forcing as the “change in net (down minus up) irradiance (solar plus long-wave; in W m^{-2}) at the tropopause AFTER allowing for stratospheric temperatures to readjust to radiative equilibrium, but with surface and tropospheric temperature and state held fixed at the unperturbed values.” The rationale for using this adjusted (instead of instantaneous) forcing is that the radiative relaxation time of the stratosphere is a few weeks, much faster than the decadal timescale for the surface-troposphere system, which is governed by the thermal inertial of the ocean [Hansen *et al.*, 1997; Shine and Forster, 1999]. Because radiative forcing for tropospheric aerosols is normally reported in the literature as the instantaneous forcing at TOA, unless otherwise noted, forcings for aerosols reported in this study are instantaneous forcings at TOA. Note that for tropospheric aerosols that only affect shortwave radiation, such as sulfate and BC, the instantaneous forcing at TOA, instantaneous forcing at tropopause, and adjusted forcing at tropopause are approximately equal [Hansen *et al.*, 1997]; therefore, no accuracy is lost in using the instantaneous forcing instead of the adjusted forcing for BC or sulfate.

Direct radiative forcing by sulfate aerosols has received much attention over the past decade. Sulfate aerosols cool the climate by scattering solar radiation, resulting in less radiative heating in the atmosphere and at the surface of the Earth. Estimates of global mean direct forcing of sulfate aerosols range between -0.29 and -0.95 W m^{-2} [Charlson *et al.*, 1991; Kiehl and Briegleb, 1993; Taylor and Penner, 1994; Boucher and Anderson, 1995; Chuang *et al.*, 1997; Feichter *et al.*, 1997; Haywood *et al.*, 1997; Penner *et al.*, 1997, 1998; Koch *et al.*, 1999; Kiehl *et al.*, 2000; Tegen *et al.*, 2000; Adams *et al.*, 2001; Ghan *et al.*, 2001]. Variabilities in the predicted global distribution of sulfate aerosols account for some of the disagreement, but differences in assumptions regarding the optical properties of sulfate aerosols play the most significant role in the wide range of estimates. Specifically, the optical properties are strongly dependent on the amount of water associated with the aerosol. Adams *et al.* [2001] showed that the calculated forcing is extremely sensitive to how the effect of water uptake on aerosol is taken into account. Also, even though nitrate and ammonium ions contribute a small amount of mass to inorganic aerosol, their influence in water uptake contributes a nontrivial mass to the total aerosol mass.

Carbon in particulate matter can take a variety of forms. Typically, these are divided into three main components: organic carbon (OC), a refractory component also known as elemental carbon (EC), and carbonate carbon (CO_3^{2-}). The split between EC and OC can be measured by different methods, but is typically obtained by measuring the amount that pyrolyzes at different temperatures. Soot generally falls in the EC fraction. For the purposes of global radiative forcing emissions inventories, BC is defined as the carbon component of particulate matter that absorbs light. Methods that measure light absorption in particulate matter assume that BC is the only light absorbing component present, while methods that rely on the partitioning of EC and OC use a somewhat arbitrary division point. For estimates of global

radiative forcing, BC is generally considered as equivalent to EC. Some components of OC may also be light-absorbing; in this case, inventories of BC and OC may overlap.

The principal source of black carbon is combustion. Except for natural fires, whose sources are small on a global basis, most black carbon derives from either biomass burning or fossil fuel combustion. The principal types of biomass burning include (1) savanna fires to clear and renew land, (2) forest fires for clearing purposes, (3) burning of agricultural waste to clear land, (4) the burning of wood to produce charcoal and (5) the burning of wood, agricultural wastes, charcoal and dung for domestic fuel. Each of these processes produces organic carbon as well, although the ratio of BC to OC in emissions varies depending on the type of fuel and the manner of burning. For example, savanna fires typically have a larger ratio of BC/OC than forest fires. This is because savanna fires typically burn in a flaming mode which enhances emissions of BC, while forest fires are a combination of flaming and smoldering. The principal sources of black carbon from fossil fuel emissions derive from diesel fuel use and coal combustion.

Black carbon is a strong absorber of visible and near-IR light; therefore, black carbon concentrations can be determined by light-absorption measurements of particles collected on filters [Lindberg *et al.*, 1999]. In contrast, aerosol organic carbon represents an aggregate of hundreds of individual compounds with a wide range of chemical and thermodynamic properties, making concentration measurements difficult using any single analytical technique. Instead, aerosol OC content is usually determined from the difference between total carbon and black carbon contents [Turpin *et al.*, 2000]. While some OC components may absorb light, most researchers assume that OC has negligible absorption of solar radiation. Particulate emission factors are generally stated for BC and OC with an aerodynamic diameter of less than or equal to $2.5 \mu\text{m}$ (PM_{2.5}). In some cases, however, the literature uses different measures, such as BC in PM_{1.0} (submicron PM), or PM₁₀ (less than or equal to $10 \mu\text{m}$.)

Organic carbon is the most abundant carbonaceous species. It may be primary if introduced directly into the atmosphere in the form of particles by various combustion and natural sources, or secondary if produced in the atmosphere by gas-to-particle conversion of anthropogenic and biogenic precursor gases. The term “organic carbon” is used to denote the total organic aerosol fraction, which is composed of a large number of individual compounds that determine the optical and CCN properties of this fraction. Both organic and black carbon affect the extinction of solar radiation. Black carbon is the principal light-absorbing aerosol species (some dust particles and condensed aromatic hydrocarbons may also contribute to light absorption), while both organic and black carbon aerosols are light-scattering species. Carbonate carbon is a constituent of mineral dust.

From a climatic point of view, organic carbon acts similarly to sulfate in that it largely scatters solar radiation and cools the Earth-atmosphere system by reflecting some portion of the incoming sunlight back to space that would otherwise reach the surface. The total global mean direct radiative forcing of organic carbon from fossil

fuel and biomass burning is estimated to be between -0.3 to -0.8 W m^{-2} [Koch, 2001; Chung and Seinfeld, 2002]. The discrepancy is due to differences in predicted total global burden and assumption of water uptake, which affects optical properties.

In contrast to sulfate and organic carbon, black carbon is a strong absorber of solar radiation. By absorbing radiation in the atmosphere and preventing that radiation from reaching the Earth's surface, black carbon has the opposite effects of warming the atmosphere but cooling the surface. If black carbon is assumed to be contained in particles physically separated from other types of aerosol, forming an external mixture, it exerts an estimated warming of 0.27 to 0.51 W m^{-2} [Chung and Seinfeld, 2002; Koch, 2001; Jacobson, 2000]. However, the overall direct radiative impact of BC depends strongly on the manner in which it is mixed with non-absorbing aerosols, such as sulfate and organic carbon [Chung and Seinfeld, 2002; Lesins et al., 2002; Jacobson, 2000; Chylek et al., 1995]. Jacobson [2000] estimates that if BC is assumed to be internally mixed with other aerosols instead of externally mixed, the globally averaged radiative forcing increases from 0.27 to 0.78 W m^{-2} . Similarly, Chung and Seinfeld [2002] estimate an increase from 0.51 to 0.8 W m^{-2} . Since BC particles are emitted from the same types of processes as those of other aerosol, e.g. with OC from biomass burning and with OC and sulfates from fossil fuel, and all aerosols undergo atmospheric processing such as gas-to-particle conversion and coagulation, BC remaining completely externally mixed in the atmosphere is unlikely. On the other hand, BC is largely immiscible with other aerosol species so that a fully internal mixture is also not likely. Jacobson [2000] suggested that BC can be represented as contained in a core surrounded by a shell of other species. Using the core model, Jacobson [2000] estimated the contribution of BC to radiative forcing to be 0.54 W m^{-2} , which is in between that of the externally- and internally-mixed cases. While the exact manner in which BC is mixed with other species is not known, and almost certainly varies globally, to determine the contribution of BC to climate forcing, BC cannot be considered independently of other aerosols.

As mentioned previously, particulate matter also affects the climate by means of indirect forcing. The uncertainty in the estimated present-day magnitude of indirect forcing is even greater than that of direct forcing. The so-called first indirect effect refers to the increase in cloud reflectivity when anthropogenic aerosols serve as cloud condensation nuclei (CCN), leading to increased cloud droplet concentration with decreased droplet sizes [Twomey, 1977]. Other types of indirect effects have been identified, such as increased cloud lifetime associated with decreased precipitation in clouds of smaller droplets [Albrecht, 1989], but these effects have yet to be studied in global simulations. The problem of estimating the indirect forcing of atmospheric aerosols is very complex as many parameters, such as aerosol size distribution and chemical composition, may be influential. An additional limitation is the cloud parameterizations in global models. Cloud formation is a complicated process which includes updraft velocities, entrainment and detrainment and other subgrid-scale processes that are difficult to accurately represent in global models with low spatial resolution. The IPCC [2001] does not state a best estimate for the indirect

Table 1: Summary of Inorganic Aerosol Model

<i>Online Tracers</i>	<i>Offline Species</i>		<i>Thermodynamics^a</i>	
	<u>Species</u>	<u>Reference</u>	<u>Gas Phase</u>	<u>Aerosol Phase</u>
H ₂ O ₂	OH, OH ₂	<i>Spivakovsky et al.</i> [2000]	NH ₃	NH ₄ ⁺
SO ₂	NO ₃	<i>Mickley et al.</i> [1999]	HNO ₃	H ⁺
SO ₄	HNO ₃	<i>Wang et al.</i> [1998]	H ₂ O	NO ₃ ⁻
MSA				SO ₄ ²⁻
DMS				HSO ₄ ⁻
NH ₃				OH ⁻
NH ₄				H ₂ O

^a Using ISORROPIA from *Nenes et al.* [1998].

forcing of anthropogenic aerosols, but gives an uncertainty range between 0 to -4.8 W m⁻².

The purpose of this study is to estimate future radiative forcing of black carbon, organic carbon, and sulfate aerosols. The values of radiative forcing, both at top of the atmosphere (TOA) and at the surface, are predicted over 25-year intervals for 2000, 2025, 2050, 2075, 2100 based on IPCC estimates of emissions over the next century.

2 Model Description

2.1 Aerosol Simulation

Simulation of aerosol processes follows that of *Adams et al.* [1999], *Adams et al.* [2001], and *Chung and Seinfeld* [2002]. Description of the model is given in the next few sections.

2.1.1 Goddard Institute for Space Studies General Circulation Model II-prime

Three-dimensional global transport of aerosols and relevant gas-phase species is simulated on-line in the Goddard Institute for Space Studies General Circulation Model II-prime (GISS GCM II-prime), which is described by *Hansen et al.* [1983]. The model solves simultaneous equations for conservation of energy, momentum, mass, water vapor, and the equation of state. The version of the GISS GCM used for this study has horizontal resolution of 4° latitude by 5° longitude with 2° latitude circles at the poles and nine σ layers in the vertical, from the surface to 10 mbar. The

vertical layers are centered approximately at 959, 894, 786, 634, 468, 321, 201, 103, and 27 mbar. The GCM surface layer is 50 mbar thick. Updates to the model include a new boundary layer parameterization that uses a scheme that incorporates a finite modified Ekman layer [*Hartke and Rind, 1997*], a new land surface model [*Rosenzweig and Abramopoulos, 1997*], and new treatment of clouds [*Del Genio and Yao, 1993; Del Genio et al., 1996*]. The GCM utilizes a fourth-order scheme for momentum advection. Tracers, heat, and moisture are advected each dynamical time step by the model winds using the quadratic upstream scheme, which is mathematically equivalent to the second-order moment method of *Prather* [1986]. *Rind and Lerner* [1996] provide a detailed discussion of the GCM relevant to tracer transport. The dynamical time step for tracer processes is 1 hour. The version of GISS GCM-II' employs monthly mean ocean temperature maps.

The current study employs the GISS General Circulation Model II'. With a $4^\circ \times 5^\circ$ global resolution, this GCM is one of the more coarsely resolved among the GCMs in use worldwide for climate studies. We have used this GCM because its coarser resolution has allowed the inclusion of aerosol physics and chemistry at a level of detail that was not heretofore possible with more highly resolved GCMs. With the increasingly faster computational facilities available in many laboratories, it has now become possible to integrate detailed aerosol physics into finer-resolution GCMs. One example is the Max Planck Institute for Meteorology in Hamburg ECHAM5-HAM [*Stier et al., 2004*].

Since the present study was initiated, GISS has completed development of the next generation version of the GCM II', which is referred to as the GISS model E [*Schmidt et al., 2005*], which has been adopted as the new standard GISS model with the present version designated as model III. Model E is a reprogrammed, modularized and documented version of prior GISS climate models including improved representations of several physical processes. *Schmidt et al.* [2005] provide extensive comparisons of the atmospheric model climatology with observations. Principal model shortcomings include $\sim 25\%$ regional deficiency of summer stratus cloud cover on the west coast of the continents with resulting excessive absorption of solar radiation by as much as 50 W m^{-2} , deficiency in absorbed solar radiation and net radiation over other tropical regions by typically 20 W m^{-2} , sea level pressure too high by 4-8 hPa in the winter in the Arctic and 2-4 hPa too low in all seasons in the tropics, deficiency of rainfall over the Amazon basin by about 20%, deficiency in summer cloud cover in the western United States and central Asia by $\sim 25\%$ with a corresponding $\sim 5^\circ\text{C}$ excessive summer warmth in these regions. *Schmidt et al.* [2005] compare simulations with $2^\circ \times 2.5^\circ$ and $4^\circ \times 5^\circ$ horizontal resolutions, finding that the climatology of the $4^\circ \times 5^\circ$ version is almost as realistic as the finer resolution in most respects.

Since the goal of the present study is global direct aerosol forcing, the GISS GCM II' is expected to be quite adequate by comparison with other more highly resolved GCMs. A next logical step would be to study climatic effects of greenhouse and aerosol forcing over the next century, especially at the spatial scale of the State of California. For this, a more highly spatially resolved GCM would be desirable.

2.1.2 Wet Deposition

Wet deposition of dissolved tracers follows the GCM treatment of liquid water, which is described by *Del Genio and Yao* [1993] and *Del Genio et al.* [1996]. The GCM distinguishes between large-scale (stratiform) and convective clouds. During in-cloud scavenging, gas-phase tracers dissolve in cloud water according to their effective Henry's law constants. Hydrophilic aerosols are assumed to be infinitely soluble, but hydrophobic aerosols are insoluble. Transport of dissolved chemical tracers follows the convective air mass, and scavenging is applied only to species within or below the cloud updraft. Moist convection includes a variable mass flux scheme determined by the amount of instability relative to the wet adiabat, two plumes, one entraining and one nonentraining, as well as compensating subsidence and downdrafts [*Del Genio and Yao*, 1993]. All liquid water associated with convective clouds either precipitates, evaporates, or detrains within the one hour GCM dynamical time step, and the dissolved chemical tracers are either deposited (in case of precipitation) or returned to the air (in case of evaporation or detrainment) in corresponding proportions. All water condensed above a certain level (typically 550 mbar) is detrained into cirrus anvils and added to the large-scale cloud liquid water content, which is carried as a prognostic variable in the GCM. For large-scale clouds, in-cloud tracers are redissolved into cloud water (using Henry's law coefficients) and scavenged according to a first-order rate loss parameterization that depends on the rate of conversion of cloud into rain water. Below both types of clouds, aerosols and soluble gases are scavenged according to a first-order parameterization that depends on the amount of precipitation [*Koch et al.*, 1999]. Dissolved tracer is returned to the atmosphere if precipitation from either type of cloud evaporates.

2.1.3 Dry Deposition

Dry deposition occurs in the lowest model layer. Deposition velocity is based on the resistance-in-series parameterization of *Wesely and Hicks* [1977]. Aerodynamic resistances are computed as a function of GCM surface momentum and heat fluxes. Surface resistances are scaled to the resistance of SO_2 , which is parameterized as a function of local surface type, temperature, and insolation [*Wesely*, 1989]. All tracers except for H_2O_2 are assumed to be nonreactive at the surface.

2.1.4 Inorganic Aerosols

On-line simulation predicts the concentrations of H_2O_2 , dimethyl sulfide (DMS), methanesulfonic acid (MSA), SO_2 , NH_3 , SO_4^{2-} , NO_3^- , NH_4^+ and aerosol water. Gas-phase reactions of DMS with OH and NO_3 radicals and oxidation of SO_2 by OH are included, as well as aqueous oxidation of SO_2 by H_2O_2 inside clouds. Monthly average three-dimensional concentration fields for NO_3 radicals are imported in the GISS GCM from the work of *Wang et al.* [1998] and five-day-average three-dimensional concentration fields for OH and OH_2 are imported from the work of *Spivakovsky et al.*

Table 2: Summary of Chemical Reactions for Modeling Inorganic Aerosols

<i>Gas Phase</i>	<i>Aqueous Phase</i>
$\text{DMS} + \text{OH} \rightarrow \text{SO}_2$	$\text{SO}_2(\text{g}) \Leftrightarrow \text{SO}_2(\text{aq})$
$\text{DMS} + \text{OH} \rightarrow 0.75\text{SO}_2 + 0.25\text{MSA}$	$\text{H}_2\text{O}_2(\text{g}) \Leftrightarrow \text{H}_2\text{O}_2(\text{aq})$
$\text{DMS} + \text{NO}_3 \rightarrow \text{HNO}_3 + \text{SO}_2$	$\text{SO}_2(\text{aq}) + \text{H}_2\text{O} \rightarrow \text{HSO}_3^- + \text{H}^+$
$\text{SO}_2 + \text{OH} \rightarrow \text{H}_2\text{SO}_4$	$\text{HSO}_3^- + \text{H}_2\text{O}_2 \rightarrow \text{SO}_4^{2-} + \text{H}_2\text{O} + 2\text{H}^+$
$\text{HO}_2 + \text{HO}_2 \rightarrow \text{H}_2\text{O}_2 + \text{O}_2$	
$\text{H}_2\text{O}_2 + h\nu \rightarrow \text{H}_2\text{O} + \text{HO}_2$	
$\text{H}_2\text{O}_2 + \text{OH} \rightarrow \text{H}_2\text{O} + \text{HO}_2$	
$\text{NH}_3 + \text{OH} \rightarrow \text{products}$	

[2000]. The concentrations are assumed to be constant for all time periods. For the purpose of determining aerosol nitrate concentrations, total nitric acid concentration fields are taken from the the Harvard-GISS GCM for the preindustrial period, 2000, and 2100 [Mickley *et al.*, 1999]. For the years 2025, and 2050, and 2075, nitric acid concentrations are interpolated linearly between the 2000 and 2100 results.

Aerosol dynamics and composition are treated with a simple bulk model (no aerosol size distribution) of internally mixed SO_4^{2-} , NO_3^- , NH_4^+ , and H_2O . This mixture is assumed to be in thermodynamic equilibrium with the gas phase. Equilibrium concentrations are calculated using the gas-particle inorganic equilibrium model ISORROPIA [Nenes *et al.*, 1998] at every dynamical time step. All chemical components of inorganic aerosol are considered to be infinitely soluble in clouds for the purpose of computing wet deposition. A summary of the inorganic aerosol modeling is given in Tables 1 and 2.

2.1.5 Carbonaceous Aerosols

Simulation of carbonaceous aerosols follows the methodology of Chung and Seinfeld [2002]. Carbonaceous aerosols included in the model are black carbon (BC) and primary organic aerosol (POA). POA are organic particles that are emitted directly into the atmosphere from fossil fuel, biofuel, and biomass burning. For the purpose of representing wet scavenging, each of these two classes of aerosol is divided into hydrophobic and hydrophilic categories, for a total of four tracers for carbonaceous aerosols. As mentioned in Section 2.1, hydrophobic aerosols are considered to be completely insoluble while hydrophilic aerosols are considered to be infinitely soluble. Of the total black carbon emitted, 80% is assumed to be hydrophobic, while 50% of the primary organic aerosol is assumed be to hydrophobic; the remaining portions are assumed be to hydrophilic [Cooke *et al.*, 1999]. Increased solubility of carbonaceous particles is generally considered to result from coating of the aerosol

Table 3: Summary of Carbonaceous Aerosol Model

<i>Tracers</i>	<i>Hydrophobic</i> → <i>Hydrophilic Conversion</i>
Hydrophobic BC	$\frac{d[\text{BC}]_{\text{hydrophobic}}}{dt} = -[\text{BC}]_{\text{hydrophobic}}e^{-t/\tau_{\text{decay}}}$
Hydrophilic BC	$\frac{d[\text{BC}]_{\text{hydrophilic}}}{dt} = +[\text{BC}]_{\text{hydrophobic}}e^{-t/\tau_{\text{decay}}}$
Hydrophobic POA	$\frac{d[\text{POA}]_{\text{hydrophobic}}}{dt} = -[\text{POA}]_{\text{hydrophobic}}e^{-t/\tau_{\text{decay}}}$
Hydrophilic POA	$\frac{d[\text{POA}]_{\text{hydrophilic}}}{dt} = +[\text{POA}]_{\text{hydrophobic}}e^{-t/\tau_{\text{decay}}}$
	$\tau_{\text{decay}}=1.15$ days

by soluble species such as sulfuric acid or sulfate. Accurate modeling of solubility would require knowledge of the rate at which ambient carbonaceous aerosols acquire a coating of hydrophilic material and also the hygroscopic behavior of the resulting particles, information that is not generally available. In the absence of such information, we adopt the estimate from *Cooke et al.* [1999], that ambient conversion of carbonaceous aerosol from a hydrophobic to a hydrophilic state occurs with an exponential decay lifetime of $\tau_{\text{decay}}=1.15$ days. A summary of the carbonaceous model is given in Table 3.

Organic aerosol can also form in the atmosphere from gas-to-particle conversion of oxidation products of volatile organic compounds (VOCs). This category of OC is called secondary organic aerosol (SOA). SOA formation has increased globally since preindustrial times due to the increase in POA, which provide the absorptive medium into which the semi-volatile oxidation products can condense. SOA is excluded from this study because its contribution to the global OC burden is relatively small [*Chung and Seinfeld, 2002*]. Also, among the VOCs, only hydrocarbons of biogenic origin are found to contribute significantly to global SOA formation. Therefore, SOAs are inherently natural, even though their concentrations increase indirectly as a result of anthropogenic activities.

2.2 Emission Scenarios

Country-specific inventories of climate change are compiled under the United Nations Framework Convention on Climate Change [*UNFCCC, 2001*]. Currently, over 180 countries subscribe to the agreement, although not all have produced climate change inventories. Climate change emissions inventories prepared under the UNFCCC generally conform with guidelines developed by the Intergovernmental Panel on Climate Change (IPCC). These inventories typically focus on the greenhouse gases (CO_2 , CH_4 , N_2O , HFC, PFC, and SF_6); however, most also include

volatile organic compounds (VOC), nitrogen oxides (NO_x), and carbon monoxide (CO) and many include other pollutants such as sulfur dioxide (SO_2). To date, the national climate change inventories do not include BC, OC, or particulate matter.

By 2004, there exist seven global or regional emissions inventories that include BC. The Global Emission Inventory Activity (GEIA) [Penner *et al.*, 1993], developed as part of the International Global Atmospheric Chemistry (IGAC) project, estimates global BC emissions in a 1° by 1° grid, for an inventory base year of 1990. Global BC inventories have also been developed by Cooke *et al.*, as part of ECHAM4 [Cooke *et al.*, 1999]; by Cooke and Wilson [1996], and by Lioussse *et al.* [1996]. Streets also developed a province-level BC emissions inventory for China as part of the CHINA-MAP project [Streets *et al.*, 2001]. Two of these inventories, ECHAM4 and Lioussse *et al.*, include OC as well as BC. Recently, Schaap *et al.* [2004] presented an updated BC emissions inventory for Europe. The global BC emissions inventory of Bond *et al.* [2004] is employed in the present study.

One important source of information on BC emissions is the body of particulate composition data developed over the last 20 years as part of “source apportionment” studies designed to identify the important emission sources contributing to elevated levels of respirable particulate matter. Many particulate matter fingerprints developed for these studies include EC which, as noted above, is considered as roughly equal to BC.

EPA’s SPECIATE database includes almost 200 measurements of the percentage of EC, OC, and other components of $\text{PM}_{2.5}$ [U.S.E.P.A., 1999]. Other sources of particulate fingerprint data include: the California Air Resources Board (CARB) speciation manual [C.A.R.B., 1999], measurements carried out under the Northern Front Range Air Quality Study [Zielinska *et al.*, 1998], and data compiled by Desert Research Institute [Chow and Watson, 1995]. BC emission factors can be estimated by applying EC speciation factors to $\text{PM}_{2.5}$ emission factors, from sources such as EPA’s Compilation of Emission Factors (AP-42) [U.S.E.P.A., 1991]. Alternatively, speciation factors can be applied directly to the $\text{PM}_{2.5}$ emissions inventories to estimate BC emissions. In addition, separate EC emissions estimates have been published for a number of emission source types as a result of fingerprint analyses. Because we rely directly on the global BC emissions inventory of Bond *et al.* [2004], it is not necessary to go through calculations such as above.

The IPCC Special Report on Emission Scenarios (IPCC SRES) [Nakicenovic and Swart, 2000] describes several emission scenarios to explore the uncertainties behind potential trends in global developments and GHG emissions. Included in the report are four scenario families that are representative of a broad range of driving forces from demographic to social and economic developments, but exclude catastrophic futures, such as large-scale environmental or economic collapses. Each family of SRES scenarios includes a descriptive part (called a “storyline”). The storylines differ in how global regions interrelate, how new technologies diffuse, how regional economic activities evolve, how protection of local and regional environments is implemented, and how demographic structure changes. Within each family are a number of al-

Table 4: Summary of Estimated Global Emissions of Aerosol Components and Gaseous Aerosol Precursors

Species	Units	Emission Rates					
		Preindustrial	Modern Day	2025	2050	2075	2100
BC	Tg yr ⁻¹	0.7	7.9	10.6	13.1	16.1	21.5
POA	Tg yr ⁻¹	3.8	33.4	44.5	55.3	67.4	88.3
SO ₂	Tg S yr ⁻¹	4.8	73.8	110	110	74.0	65.1
NH ₃	Tg N yr ⁻¹	18.2	55.5	75.6	87.5	102	116
DMS	Tg S yr ⁻¹	26.0	26.0	26.0	26.0	26.0	26.0

ternative interpretations on global and regional developments and their implications for GHG, ozone precursors, and sulfur emissions. Each of these scenarios is consistent with the broad framework specified by the storyline of the scenario family. All four SRES “futures” represented by the distinct storylines are treated as equally possible and there are no “best guess”, “central”, “business-as-usual”, “surprise”, or “disaster” futures.

To project how global aerosol radiative forcing might change as the current century progresses, six different time periods have been simulated: preindustrial (roughly corresponding to the year 1800), modern day (year 2000), and the years 2025, 2050, 2075, and 2100. According to the IPCC [2001], emission scenario A2 represents middle of the road in terms of anthropogenic radiative forcing; therefore, emission scenario A2 is chosen for this study to provide the “central” estimates for anthropogenic aerosol radiative forcing. The A2 storyline and scenario family describes a very heterogeneous world. The underlying theme is self-reliance and preservation of local identities. Fertility patterns across regions converge very slowly, which results in high population growth. Economic development is primarily regionally oriented and per capita economic growth and technological change are more fragmented and slower than in other storylines. A summary of the emissions of all relevant species for all time periods is given in Table 4 and shown in Figure 1.

Anthropogenic sulfur emissions for the modern day and the future are prescribed based on the IPCC SRES A2 emission scenario. Preindustrial sulfur emissions include only DMS from the oceans and volcanic SO₂ emissions. Since atmospheric DMS is biogenic in origin, DMS emissions are assumed to be the same for all time periods. Volcanic emissions of SO₂ are also assumed to be constant. Note that, as indicated in Figure 1, SO₂ emissions are predicted to increase from 2000 to 2025, and then to decrease after 2050 due to sulfur emission control policies.

Ammonia emissions are based on the Global Emissions Inventory Activity (GEIA) [Bouwman *et al.*, 1997], which provides estimated emissions for the year 1990. Natural emissions of ammonia from the oceans, undisturbed soils, and wild animals are

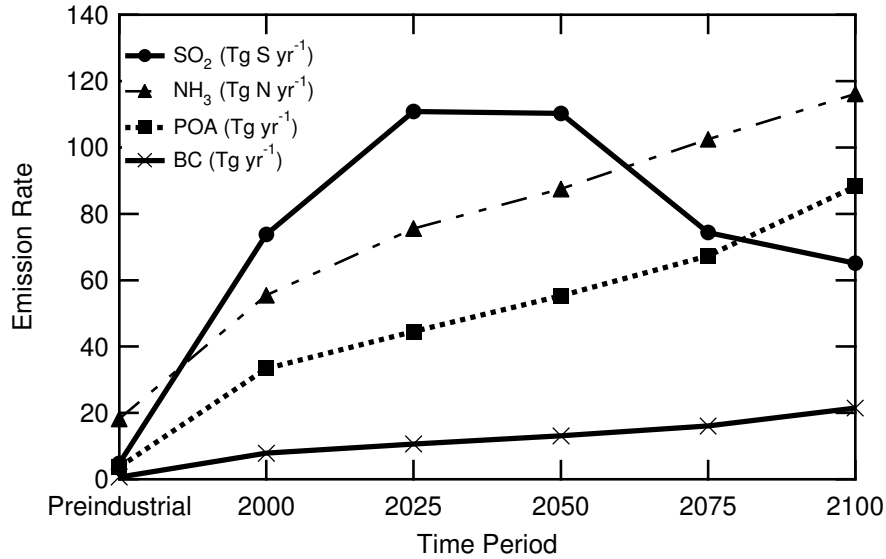


Figure 1: Estimated global emissions of aerosol components and gaseous aerosol precursors.

assumed to be unchanged from preindustrial time to 2100. Emissions from synthetic fertilizers, industrial processes, and fossil fuel are assumed to be zero for the preindustrial period. Similar to carbonaceous aerosols, preindustrial biomass emissions of NH₃ are set to 10% of the modern day level. Emissions from livestock, crops, humans, and pets are assumed to be proportional to human population, which is taken to be 20% of the present day value in 1800. Since agriculture is the main anthropogenic source of both N₂O and ammonia emissions, anthropogenic emissions for the years 2000 to 2100 are scaled with the N₂O emissions prescribed in the IPCC SRES A2 scenario.

For the year 2000, annual emissions of black carbon and primary organic aerosols are taken from the emission inventory of *Bond et al.* [2004], with estimated present-day global BC emission rates being 1.6, 3.3, and 3.0 Tg yr⁻¹ for biofuel, open burning, and fossil fuel, respectively. *Bond et al.* [2004] provide only annual emissions; the biomass burning inventory is distributed monthly by scaling the annual emissions by monthly fire counts of the Global Burned Area 2000 Project [*Grégoire et al.*, 2003]. Fossil fuel and biofuel emissions are assumed to be constant throughout the year.

For preindustrial carbonaceous aerosol emissions, only 10% of the modern day global emission from open biomass burning is assumed to occur in the preindustrial period. Preindustrial biofuel emissions are assumed to be 20% of the modern level based on population proxy. Fossil fuel sources are neglected for the preindustrial period. With the lack of future emission scenarios for carbonaceous aerosols and

following the method of the IPCC Assessment Report, future emission inventories for carbonaceous aerosols are constructed by using the ratio of the source strength of CO in 2025, 2050, 2075, and 2100. Future emission inventories for CO are given by SRES. Because IPCC SRES emission scenarios for CO do not provide a breakdown of CO emissions by source category, the use of scaling implicitly assumes that the ratio of emission of CO by biomass burning and by fossil fuel burning remain roughly constant.

2.3 Direct Radiative Forcing and Aerosol Optical Properties

Direct radiative forcing is calculated as the difference in the solar irradiance at the top of atmosphere (TOA) and at the surface with and without the presence of aerosols. Longwave forcing is neglected as it is expected to be small for the aerosols studied here [Haywood *et al.*, 1997]. The forcing is calculated on-line using the radiation model embedded in the GISS GCM [Lacis and Hansen, 1974; Hansen *et al.*, 1983; Lacis and Mishchenko, 1995; Tegen *et al.*, 2000]. Reflection, absorption, and transmission by aerosols are calculated using the single Gauss point doubling/adding radiative transfer model. The correlated k -distribution method is used to compute absorption by gases for 6 solar and 25 thermal intervals [Lacis and Oinas, 1991]. The radiation time step in the model is 5 hours. The radiative forcing calculations do not feed back into the GCM climate, so that the same meteorological fields are used for all time periods.

A total of six simulations are carried out to calculate direct radiative forcing, one for each of the year 1800 (preindustrial), 2000, 2025, 2050, 2075, and 2100 using the emissions inventories described in Section 2.2. For each simulation, online aerosol concentrations are calculated following the methodology described in Section 2.1. Direct radiative forcing is calculated online during each simulation by making five calls to the radiation scheme at each radiation time step (5 hours). During all calls to the radiation scheme and for all years, greenhouse gas concentrations are kept constant at the 1980s level (340 ppm of CO₂ and 1.6 ppm of CH₄). For the first call to the radiation scheme, online concentrations of SO₄²⁻/NH₄⁺/NO₃⁻/H₂O aerosol are used for the shortwave radiative flux calculations. Online concentrations of OC are used for the second call the radiation scheme. Then online concentrations of BC are used for the third call the radiation scheme. In the fourth call, online concentrations of SO₄²⁻/NH₄⁺/NO₃⁻/H₂O, OC, and BC are all used and the aerosols are assumed to be internally mixed. For the first four calls to the radiation scheme, the radiative fluxes are archived for diagnostics and do not affect the climate simulation. Finally, in the fifth call to the radiation scheme, no aerosol is included in the radiative flux calculations. The radiative forcings of SO₄²⁻/NH₄⁺/NO₃⁻/H₂O, OC, BC, and the internal mixture are calculated as the differences in shortwave fluxes of the first, second, third, and fourth and those of the fifth calls to the radiation scheme, respectively. Radiative forcing for the external mixture of SO₄²⁻/NH₄⁺/NO₃⁻/H₂O, OC, and BC is the arithmetic sum of the radiative forcings of SO₄²⁻/NH₄⁺/NO₃⁻/H₂O, OC, and BC.

Anthropogenic contributions to direct radiative forcings are calculated as the differences between radiative forcings of the aerosol in the year 2000, 2025, 2050, 2075, 2100 and those of the preindustrial period.

As pointed out earlier, the mixing state of black carbon with other aerosols is important in determining its radiative effect [Chýlek *et al.*, 1995; Haywood *et al.*, 1997; Myhre *et al.*, 1998; Jacobson, 2000]. To bound the impact of aerosol mixing state on direct radiative forcing, two limiting cases are considered. In one case, each aerosol component (sulfate, organic carbon, black carbon) is assumed to be contained in physically separate particles, forming an external mixture. In the other case, each particle consists of a homogeneous mixture of all species present, i.e. the aerosols are internally mixed. An alternative microphysical representation is to treat each particle that contains black carbon, organic carbon, and sulfate as a core of black carbon surrounded by a shell of sulfate, OC, and water. As shown by Jacobson [2000], the radiative forcing of aerosols that consist of such a core-shell model lies between those of fully internally- and externally- mixed particles. By considering the two extreme cases, we can estimate the range of radiative forcing values attributed to black carbon together with other aerosol species.

Optical properties (extinction efficiency, single-scattering albedo, and asymmetry parameter) of the aerosols are determined by Mie theory based on wavelength-dependent refractive indices and assumed size distributions [Bohren and Hu man, 1983]. Following the recommendation of Lacis and Mishchenko [1995], the particle size distribution is assumed to be the standard gamma distribution given by

$$n(r) = \frac{(ab)^{(2b-1)/b}}{\Gamma[(1-2b)/b]} r^{(1-3b)/b} \exp[-r/(ab)] \quad (2)$$

where $n(r)dr$ is the fraction of the particles with radii from r to $r + dr$, Γ is the gamma function, and a and b are constants. One can show that the distribution parameters a and b are equal to the area-weighted effective radius r_e and the effective variance v_e , respectively, i.e.

$$a = r_e = \frac{\int_0^\infty r^2 n(r) dr}{\int_0^\infty r^2 n(r) dr} \quad (3)$$

and

$$b = v_e = \frac{\int_0^\infty (r - r_e)^2 r^2 n(r) dr}{\int_0^\infty r^2 n(r) dr} \quad (4)$$

As explained in Lacis and Mishchenko [1995], the key parameter that best describes the radiative properties of a given size distribution is the cross-section weighted effective radius r_e , which is listed in Table 5 for each of the the aerosol type studied here. We assume that the effective variance is constant at $v_e = 0.2$ even when particles take up water and grow to larger sizes [Tegen *et al.*, 2000]. The assumed effective dry radius and density, and calculated optical properties of dry aerosols

Table 5: Aerosol Physical and Optical Properties at $\lambda=550$ nm in the Dry State.

Aerosol Type	$r_{e,\text{dry}}$ (μm)	ρ (g cm^{-3})	σ_e ($\text{m}^2 \text{g}^{-1}$)	ω	g
$\text{SO}_4^{2-}/\text{NH}_4^+/\text{NO}_3^-/\text{H}_2\text{O}$	0.3	1.8	4.2	1.00	0.69
OC	0.5	1.8	2.5	0.94	0.68
BC	0.1	1.0	12.5	0.38	0.47
internal mixture	0.3

$r_{e,\text{dry}}$ = effective dry radius; *Tegen et al.* [2000].

ρ = density; *d'Almeida et al.* [1991].

From Mie scattering calculations: σ_e = extinction coefficient; ω = single scattering albedo; g = asymmetry factor.

at $\lambda=550$ nm of each class are listed in Table 5. The calculated optical properties are also plotted in Figure 2 as a function of wavelength. For all dry components of the $\text{SO}_4^{2-}/\text{NH}_4^+/\text{NO}_3^-/\text{H}_2\text{O}$ aerosol, refractive indices of ammonium sulfate from *Toon et al.* [1976] are used. Composite refractive indices of the aqueous aerosol are the volume-averaged refractive indices of ammonium sulfate and water. Refractive indices of water are taken from *d'Almeida et al.* [1991]. Refractive indices of soot in *d'Almeida et al.* [1991] are used for BC. Externally mixed BC is assumed to remain dry for the purpose of optical property calculations, even if the aerosol is hydrophilic. For externally-mixed BC, the assumption of zero water-uptake by BC will underestimate the radiative forcing of BC. For BC internally mixed with sulfate, the water-uptake by BC is negligible compared to the aerosol water associated with sulfate. For an internal mixture of BC, OC, and $\text{SO}_4^{2-}/\text{NH}_4^+/\text{NO}_3^-/\text{H}_2\text{O}$ aerosols, the refractive indices are calculated by volume-weighting the refractive indices of BC, OC, ammonium sulfate, and water.

In the absence of data for OC, refractive indices for “water-soluble” aerosol from *d'Almeida et al.* [1991] are used for OC. “Water-soluble” aerosols as described in *d'Almeida et al.* [1991] include sulfates, nitrates, as well as water-soluble organic aerosols. Water uptake by OC is also assumed to be the same as the water-soluble aerosols given in *d'Almeida et al.* [1991]. Below 50% relative humidity, water-uptake is assumed to be zero. Above 99%, the growth factor $f_g = r_{\text{wet}}/r_{\text{dry}}$ is capped at 2.52. This treatment of water uptake is similar in magnitude to that given by *Fitzgerald* [1975] and is considered to be the upper bound since not all organic compounds are as soluble as ammonium sulfate. For the case of internally mixed aerosols, the total amount of water uptake is equal to that of the externally mixed aerosols.

The radiative forcing results are highly dependent on the optical properties of

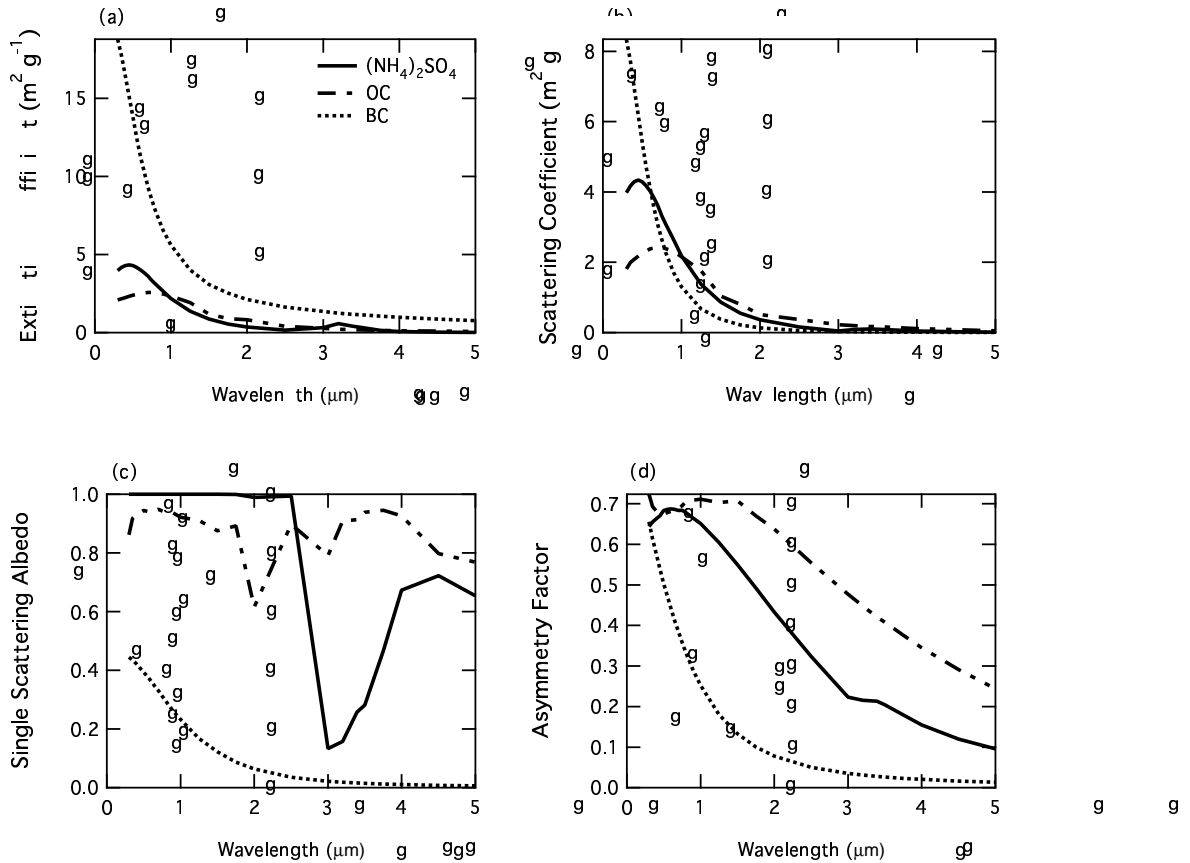


Figure 2: Wavelength-dependent optical properties for aerosols in the dry state.

aerosols, and inexact optical properties are a source of uncertainties in radiative forcing calculations. Errors in optical properties can originate from two sources. First, the wavelength-dependent refractive indices of pure aerosol component are not well characterized. For example, the data of soot refractive indices used for this study from *d’Almeida et al.* [1991] are different from those reported by *Nilsson* [1979]. Another source of uncertainties in the optical properties come from the aerosol size distribution and shape. The aerosol extinction and absorbing efficiencies are based on Mie-scattering theory, which requires knowledge of aerosol size distributions and applies to spherical particles only. The size distribution and shape of BC in the atmosphere is variable depending on the source of BC and atmospheric processing. *Bond and Bergstrom* [2004] indicate that most variations in model predicted direct radiative forcing of BC can be explained by differences in optical properties and estimated particle lifetime.

2.4 Indirect Radiative Forcing

Several types of aerosol indirect effects have been identified, either observationally or in theory, based on the various mechanisms through which aerosols perturb cloud albedo. *Twomey* [1977] and *Twomey et al.* [1984] identified the first indirect effect in which increased cloud condensation nucleus (CCN) concentrations result in increased cloud droplet concentrations, smaller drop radii, and more reflective clouds. The Twomey effect, which is the only indirect effect considered by the IPCC [2001], assumes there are no aerosol-induced changes in cloud liquid water or cloud fraction. Relaxing this assumption allows a number of secondary indirect effects in which cloud albedo is changed through changes in liquid water content or cloud fraction [*Albrecht*, 1989; *Boers and Mitchell*, 1994; *Pincus and Baker*, 1994]. Many uncertainties in cloud activation lie in the role of aerosol chemistry [*Nenes et al.*, 2002a]. Black carbon aerosol may also play an important role in indirect forcing, as solar heating can affect clouds through an alteration of the CCN spectrum [*Conant et al.*, 2002; *Nenes et al.*, 2002b] or by eliciting dynamical responses in the atmosphere that reduce cloudiness [*Hansen et al.*, 1997; *Ackerman et al.*, 2000]. Aerosol-cloud interactions can also effect climate changes by redistributing radiative and latent heating either vertically or regionally [*Ramanathan et al.*, 2001; *Roderick and Farquhar*, 2002]. These aerosol effects on precipitation have an influence on the hydrological cycle that is independent of the TOA forcing normally used as the metric of climate forcing.

Our understanding of the indirect effects can be represented through models that simulate aerosol-cloud-climate interactions on scales ranging from cloud parcel models (meters) to cloud resolving models (kilometers) and ultimately to GCMs (global). The test of our understanding will come through evaluation of the faithfulness of these models to observations. Because spatio-temporal coarseness of GCMs does not allow for simulation of the full range of scales involved in aerosol-cloud-climate interactions, this strategy requires detailed process models as a basis for simpler, larger-scale parameterizations [*Nenes and Seinfeld*, 2003]. The process models are most rigorously tested in closure studies, in which detailed observations are made of each dependent and independent variable in the model to test its accuracy over a wide range of conditions. Ultimately, the full hierarchy of aerosol-cloud-climate models must be evaluated against observations.

Direct evidence for indirect effects (such as observed correlations between cloud albedo and aerosol) are difficult to discern in satellite observations because the predicted albedo perturbation is small relative to the strong spatio-temporal variability of cloud properties. Despite these difficulties, evidence of the Twomey effect has been suggested by several satellite studies that show compelling correlations between aerosol and cloud properties. The most clear relationship is a decrease in effective radius at cloud top in regions of high aerosol column burden [*Nakajima et al.*, 2001; *Bréon et al.*, 2002; *Schwartz et al.*, 2002; *Harshvardhan et al.*, 2002]. *Nakajima et al.* [2001] sees a correlation between column aerosol and cloud optical depth, which is a more direct measure of the effect on cloud albedo. Clouds forming downwind of lo-

calized aerosol sources are seen to suppress precipitation [Rosenfeld, 2000]. However, the secondary indirect effects on cloud fraction and liquid water path remain elusive from the satellite observations. Analysis of satellite observations show little relationship [Nakajima *et al.*, 2001] or a regionally variable one [Han *et al.*, 2002]. Coakley and Walsh [2002], using AVHRR data, found that ship tracks are most often associated with a 15%-20% decrease in cloud liquid water, resulting in a small or negligible change in albedo relative to the unperturbed cloud. Even though this result may be an artifact related to aerosol-induced changes in cloud fraction [Ackerman *et al.*, 2003], the aerosol impact on cloud structure is clear from these ship track studies.

The aerosol properties that control cloud albedo, such as CCN spectrum, are not directly observed in satellite studies, but are instead retrieved from variations in estimated cloud drop concentration [Han *et al.*, 2002], predicted from transport models [Schwartz *et al.*, 2002; Harshvardhan *et al.*, 2002], or obtained from non-coincident, non-vertically resolved satellite retrievals [Nakajima *et al.*, 2001; Bréon *et al.*, 2002]. Likewise, statistical relationships found between aerosol and cloud properties may be influenced by meteorological patterns that are correlated with aerosol transport. This is particularly important, as variations in cloud dynamics (e.g. updraft velocity at cloud base, cloud top entrainment, subsidence strength) can exhibit a larger influence on cloud microphysics than variations in aerosol concentration [Leaitch *et al.*, 1996]. Several satellite studies derive liquid water path and cloud drop concentration (or effective radius and cloud optical depth) from visible and near-infrared reflectances. One problem with this strategy is that near-infrared reflectance is only sensitive to the uppermost ~ 100 m of the cloud, whereas visible reflectance is retrieved for the entire cloud column. Calculations from such measurements are subject to errors related to assumptions about the vertical distribution of cloud microphysics, the dispersion of the cloud drop distribution (which is known to be influenced by aerosol), and layers of aerosol above cloud. Brenguier *et al.* [2000] and Brenguier and Fouquart [2000] use aircraft observations to show that simple representations of N. Atlantic marine stratocumulus are accurate enough for certain retrieved properties; however, it has not been demonstrated that this result is general.

The CCN spectrum, or supersaturation spectrum, is a fundamental property of an aerosol population that describes the number of particles that are unstable to condensational growth at a given ambient supersaturation of water vapor. Studies attempting to reconcile observed size distributions with observed CCN spectra or concentrations of CCN for a fixed value of supersaturation have met with varying degrees of success. Chuang *et al.* [2000] and Cantrell *et al.* [2001] present reviews of prior studies.

A large source of uncertainty in previous studies may lie in the role of chemical properties of particles, especially those containing organic species [Charlson *et al.*, 2001; Nenes *et al.*, 2002a]. Many aerosol-CCN comparisons implement Köhler theory using chemical properties assuming the particles are a mixture of a pure soluble salt, such as ammonium sulfate or sodium chloride, and insoluble material [Twomey, 1959; Hudson and Da, 1996; Rivera-Carpio *et al.*, 1996; Liu *et al.*, 1996; Cantrell *et al.*,

2000, 2001]. In these studies, organic aerosols are neglected [Hudson and Da, 1996], treated as equivalent to a soluble salt [Rivera-Carpio *et al.*, 1996], or treated as completely insoluble [Chuang *et al.*, 2000; Cantrell *et al.*, 2000, 2001]. Theoretical and laboratory studies indicate that organics may alter the activation characteristics of aerosol by reducing the mass accommodation coefficient of water [Bigg, 1986; Saxena *et al.*, 1995; Feingold and Chuang, 2002] or by decreasing droplet surface tension [Facchini *et al.*, 1999]. Partially soluble aerosols [Shulman *et al.*, 1996] and soluble gases [Laaksonen *et al.*, 1998] may also contribute to uncertainties in the predictions of Köhler theory when the concentrations or properties of such species are unknown.

Simple parcel theory predicts that number concentration within adiabatic cloud regions is determined within tens of meters above cloud base, and that cloud liquid water throughout the column is controlled by thermodynamic processes. For regions of stratocumulus clouds that remain adiabatic, cloud drop effective radius has been predicted to within 15% of observations from an adiabatic model, meaning that horizontal mixing is not important in these regions [Pawlowaska and Brenguier, 2000]. In regions where cloud liquid water is sub-adiabatic, homogeneous mixing processes reduce effective radius and inhomogeneous mixing processes reduce number concentration; the relative importance of homogeneous and inhomogeneous mixing is not well constrained. Observations of marine stratocumulus [Pawlowaska and Brenguier, 2000] and trade cumulus [Conant *et al.*, 2004] indicate that in most cloud regions, inhomogeneous mixing appears to dominate over homogeneous mixing. However, Conant *et al.* [2004] and others find that droplet dispersion increases with mixing, indicating that more complex processes are involved.

An expected consequence of decreased cloud drop radius is the suppression of precipitation, which can increase cloud liquid water and decrease net latent heating [Albrecht, 1989]. Evidence indicates that initiation of collision-coalescence precipitation formation requires effective radii larger than about 15 μm [Gerber, 1996], and that precipitation is suppressed in clouds with high droplet concentrations relative to clouds of the same thickness with lower droplet concentrations [Rosenfeld and Lensky, 1998; Ferek *et al.*, 2000; Rosenfeld, 2000]. Collision-coalescence is also influenced by cloud drop dispersion, which is sensitive to both aerosol properties and cloud dynamics.

2.4.1 Sulfate Indirect Forcing

A total of six simulations are carried out to calculate indirect radiative forcings for sulfate aerosol, one for each of the year 1800 (preindustrial), 2000, 2025, 2050, 2075, and 2100 using the emissions inventories described in Section 2.2. For each simulation, online aerosol concentrations of SO_4 are calculated following the methodology described in Section 2.1. Using online concentrations of SO_4 , the cloud optical depth is calculated as described in the next two paragraphs. Indirect radiative forcing is calculated online during each simulation by making two calls to the radiation scheme

at each radiation time step. During the first call to the radiation scheme, calculated cloud optical depths based on SO_4 concentrations are used for the shortwave radiative flux calculations. The radiative fluxes calculated during the first call to the radiation scheme are archived for diagnostics and do not affect the climate simulation. During the second call to the radiation scheme, cloud optical depths calculated by the baseline case of the GISS GCM are used. The GISS GCM assumes that the cloud droplet concentrations are constant at $N_d = 60 \text{ cm}^{-3}$ over ocean and $N_d = 170 \text{ cm}^{-3}$ over land. Anthropogenic contributions to sulfate indirect radiative forcing are calculated as the difference in shortwave fluxes of the first call to the radiative scheme of the years 2000, 2025, 2050, 2075, and 2100 and those of the preindustrial period.

The cloud droplet number concentration (N_d, cm^{-3}) is calculated as function of the sulfate concentrations ($m_{\text{SO}_4}, \mu\text{g m}^{-3}$) as given by the empirical correlations of *Boucher and Lohmann [1995]*:

$$N_d = 10^{2.21+0.41 \log_{10}(m_{\text{SO}_4})} \quad \text{Continental} \quad (5)$$

$$N_d = 10^{2.06+0.48 \log_{10}(m_{\text{SO}_4})} \quad \text{Marine} \quad (6)$$

Given that in the atmosphere anthropogenic sulfate is not the only source of cloud condensation nuclei, we assume minimum cloud droplet number concentrations of 70 cm^{-3} and 40 cm^{-3} for continental and marine air masses, respectively. These values are consistent with the measurements reported in *Boucher and Lohmann [1995]*.

Once the cloud droplet number concentration is known, the mean volume cloud droplet radius r_{vol} is calculated by

$$r_{\text{vol}} = \left(\frac{3L_{\text{WC}}}{4\pi\rho_{\text{water}}N_d} \right)^{1/3} \quad (7)$$

where L_{WC} is the cloud liquid water content (mass of water per mass of air), which is provided by the GCM, and $\rho_{\text{water}} = 1 \text{ g cm}^{-3}$ is the density of liquid water. The radiative property of cloud size distribution is best described by the area-weighted effective radius r_e , which is related to the mean volume radius by

$$r_{\text{vol}}^3 = \kappa r_e^3 \quad (8)$$

where κ is estimated to 0.67 and 0.80 for continental and marine air masses, respectively [*Martin et al., 1994*]. Finally, the cloud optical depth is

$$\tau_{\text{cloud}} = \frac{3L_{\text{WP}}}{2\rho_{\text{water}}r_e} \quad (9)$$

In the above equation, the liquid water path L_{WP} (mass of water per unit area) is provided by the GCM.

One can see from Equations 5 to 9 that as human activities increase sulfate concentration m_{SO_4} , cloud droplet number N_d increases, leading to decreased mean

volume radius r_{vol} and effective radius r_e and increased cloud optical depth τ_{cloud} . Increased cloud optical depth means that more solar radiation is reflected back to space, cooling the atmosphere. As in the case of direct radiative forcing, indirect radiative forcing is calculated as the difference in the solar irradiance at the top of atmosphere (TOA) and at the surface with and without the presence of sulfate.

2.4.2 Effect of Black Carbon on Indirect Forcing

The specific aspect of indirect climate forcing of aerosols that is of interest here is to estimate the indirect forcing attributable to black carbon aerosols. When initially emitted into the atmosphere, black carbon particles are assumed in most current studies to be hydrophobic. By definition, hydrophobic particles will not act as cloud condensation nuclei and therefore do not contribute to aerosol indirect forcing. It is generally assumed that black carbon particles become coated with hydrophilic material as they age in the atmosphere through condensation of gases, principally sulfuric acid and volatile organics. The condensing material is generally taken to be sulfate because of the large amount of sulfate in the atmosphere. Organic material may also condense on black carbon particles to render them somewhat water-soluble, although the solubility properties of organic material in the atmosphere are less well established than those of sulfate. Once black carbon becomes coated with a soluble material, the resulting composite particle may act as a CCN; only in this way may black carbon play a role in indirect forcing. To fundamentally separate out the indirect global climatic effects of black carbon aerosols from those of other aerosols, such as sulfate and organics, one must employ a GCM that simulates both particle number and mass distributions and treats black carbon particles explicitly. In so doing, it would be possible to track the number of particles introduced into the atmosphere as pure black carbon and then how these particles subsequently become hydrophilic through accretion of soluble material. It would then be possible to determine the additional number of atmospheric CCN that arise from black carbon particle emissions.

The approach that is still most widely used to model indirect aerosol forcing on a global scale is to employ empirical relationships between cloud droplet number concentration and aerosol sulfate mass [*IPCC*, 2001]. Using this approach, sulfate aerosols are implicitly assumed to control indirect aerosol forcing. If black carbon happens to be present in the sulfate particles as a result of atmospheric processing, that black carbon acts simply as an insoluble inclusion in the particle. Since sulfate is highly water-soluble and most sulfate particles are generally large enough to act as CCN, the effect of the insoluble inclusion on the CCN behavior of the particles is insignificant.

Hansen et al. [2005] have investigated the efficacies of the first and second aerosol indirect effects, AIE_1 and AIE_2 , via parameterizations that are included as options in GISS GCM Model III. They define AIE_1 and AIE_2 as the change in cloud albedo and the change in cloud area, respectively, due to an imposed change of aerosol amount. Thus, AIE_1 corresponds nominally to the *Twomey* [1977] effect of increased cloud

albedo due to an imposed increase of cloud condensation nuclei with resulting smaller cloud droplets and larger cloud optical depth, and AIE₂ corresponds nominally to the *Albrecht* [1989] effect of increased cloud cover due to an imposed increase of cloud condensation nuclei with resulting smaller cloud drops, reduced precipitation, and increased cloud lifetime. AIE₁ and AIE₂ so defined are observable as cloud albedo per unit cloud area and cloud cover, respectively. *Hansen et al.* [2005] argue that empirical data suggest AIE₂ to be the dominant aerosol indirect effect.

Empirical data support both AIE₁ and AIE₂ effects, but their global magnitudes are uncertain. IPCC [2001] concluded only that the global forcings each lie somewhere between negligible and comparable in magnitude, but opposite in sign, to the forcing by anthropogenic CO₂. *Hansen et al.* [2005] use a parameterization of aerosol indirect effects for low-level stratiform clouds, based in part on more complete aerosol-cloud modeling, to investigate indirect aerosol forcing.

The parameterization is based on observed empirical effects of aerosols on cloud droplet number concentration (N_d) [*Menon and Del Genio*, 2004]. They include four time-variable aerosols: sulfate (S), nitrate (N), black carbon (BC), and organic carbon (OC), with the distributions and histories of each of these based on simulations of *Koch et al.* [1999] and *Koch* [2001]. They multiply cloud cover (C_c) and optical depth (C_d), computed by the climate model without aerosol

$$C_c : 1 + C_2 \times \Delta N_d \times V_f \quad (10)$$

$$C_d : 1 + C_1 \times \Delta N_d \times V_f \quad (11)$$

C_1 and C_2 are constants, ΔN_d is the change of cloud droplet number concentration due to added aerosols (relative to the control run for 1880), and V_f specifies the apportionment of N_d (and thus cloud cover change) among model layers. Thus C_1 and C_2 determine the magnitude of the first and second indirect effects, ΔN_d determines the geographical distribution and temporal variations, and V_f determines the vertical distribution. V_f was obtained from interactive aerosol-cloud simulations of *Menon and Del Genio* [2004]. ΔN_d is computed from the number of added aerosols in the region of low clouds in the GISS model, i.e., at altitudes below the 720 hPa level, which comprises the lowest six layers in the GISS 20-layer model. ΔN_d is obtained by computing N_d for the control run and experiment aerosol distributions, using in both cases the empirical result from *Gultepe and Isaac* [1999]

$$N_d = 163 \log_{10}(N_a) - 273 \quad \text{Marine} \quad (12)$$

$$N_d = 298 \log_{10}(N_a) - 595 \quad \text{Continental} \quad (13)$$

where N_a is the number concentration of soluble aerosols (cm⁻³).

Active (soluble) aerosol numbers were obtained from aerosol masses with the assumption that the soluble fractions were 0.6/0.8, 0.8, 1, 1, 1, and densities were 1, 1, 1.77, 2, and 1.7 g cm⁻³ for BC, OC, sulfate, sea salt, and nitrate, respectively. The BC soluble fraction was 0.6 for industrial (fossil fuel) BC and 0.8 for outdoor biomass

burning BC. Mean particle sizes were taken as radius $0.052 \mu\text{m}$ over land and $0.085 \mu\text{m}$ over ocean for all particles except sea salt, whose mean radius was taken as $0.44 \mu\text{m}$. C_1 and C_2 were chosen to give the correct global magnitudes for the first and second indirect effects. Detailed aerosol-cloud-climate models yield a wide range for the indirect effects, from very small values to several W m^{-2} for aerosol changes from the preindustrial era to the present [IPCC, 2001]. Hansen *et al.* [2005] suggest that the most relevant global constraints are those provided by (1) widespread observations of damping of the amplitude of the diurnal cycle of surface air temperature [Hansen *et al.*, 1995], and (2) near-global satellite observations of the polarization of reflected sunlight interpreted with the aid of a global aerosol transport model [Lohmann and Lesins, 2002; Quass *et al.*, 2004]. Together these constraints suggest that the AIE is $\sim -1 \text{ W m}^{-2}$ and that it is caused predominately by AIE₂. Recent multi-spectral multi-angle satellite observations of reflected sunlight [Kaufman *et al.*, 2004] provide support for the inference that AIE₂ is the predominant indirect forcing. Hansen *et al.* [1995] use observations of changes in the amplitude of the diurnal surface air temperature cycle, in combination with global climate model simulations, to infer a non-climatic increase of low cloud cover occurring predominately over land areas. They infer AIE $\sim -1 \text{ W m}^{-2}$ for the industrial era with AIE = $-0.75 \pm 0.25 \text{ W m}^{-2}$ for the second half of the twentieth century, a period including 70% of anthropogenic forcings, with most of this forcing due to an increase of low cloud cover. Satellite measurements of the polarization of sunlight reflected by clouds are used by Lohmann and Lesins [2002] and Quass *et al.* [2004] to constrain aerosol-cloud models. Their analyses suggest that AIE₁ + AIE₂ $\sim -0.85 \text{ W m}^{-2}$, with no numerical breakdown but with AIE₂ providing a substantial part of that forcing. Kaufman *et al.* [2004] use recent observations of the satellite instruments MODIS and MISR to infer that AIE probably is primarily due to AIE₂. The Hansen *et al.* [2005] first transient simulation for 1880-2003 employs AIE₂ $\sim -1 \text{ W m}^{-2}$ and AIE₁ = 0 .

Based on these empirical analyses Hansen *et al.* [2005] chose values of C_1 and C_2 that yield forcings of the order of -1 W m^{-2} . They found that $C_1 = 0.007$, $C_2 = 0$ yields a forcing AIE₁ $\sim -0.77 \text{ W m}^{-2}$ and $C_1 = 0$, $C_2 = 0.0036$ yields AIE₂ $\sim -1.01 \text{ W m}^{-2}$ for the assumed 1880-2000 aerosol changes in the GISS model.

Of critical interest to the present study is to associate the portions of the indirect aerosol effect with each aerosol type. Because of the complexity of aerosols, with internal and external mixtures of various compositions and the idealized representations of aerosols in climate models, it is not possible at present to accurately apportion the indirect effect. Nevertheless, Hansen *et al.* [2005] make an idealized apportionment of the indirect effect among aerosol types. Their computation includes sulfates, nitrates, black carbon and organic carbon as aerosols. They carry out climate simulations, in which they remove individually the indirect effect of each of the four time-variable aerosols. This was done by retaining the direct effect of all aerosols, but excluding a specific aerosol from calculation of the aerosol indirect effect on clouds. The results of such a run were then subtracted from the results of the run that included the full direct and indirect effects of all aerosols. Only the effect

of aerosols on cloud cover was considered, but its forcing (-1.01 W m^{-2}) was such as to approximate the estimate for the total aerosol indirect effect.

Hansen et al. [2005] conclude that with the external mixing assumption the aerosol indirect effect is apportioned as sulfates (36%), organic carbon (36%), nitrates (22%), black carbon (6%). But they caution that this estimate, the first of its type, is highly uncertain. It should also be noted that the calculations of *Hansen et al.* [2005] are not applicable for internal mixtures of aerosols.

The small contribution of black carbon to aerosol indirect forcing computed by Hansen et al. is consistent with an assessment based on aerosol mixing state and the role of BC-containing particles acting as cloud condensation nuclei. *Therefore, for the purposes of the present study, we conclude that indirect aerosol forcing by black carbon is essentially negligible. Stated differently, the level of indirect aerosol forcing by black carbon is of a sufficiently small magnitude that it lies well within the uncertainty bounds of a number of the more important input parameters, such as emissions and atmospheric mixing state.*

3 Results

3.1 Global Aerosol Burdens and Concentrations

A summary of predicted global aerosol burdens is listed in Table 6 and shown in Figure 3. For both BC and POA, the global burden scales linearly with emissions as the lifetime of both types of aerosols are approximately 7 days regardless of the emission rates. The global burden of POA is 4 times as large as that of BC. For $\text{SO}_4^{2-}/\text{NH}_4^+/\text{NO}_3^-/\text{H}_2\text{O}$ aerosol, the global burden is dominated by water, indicating the importance of accurately determining the water content associated with SO_4 , NO_3 , and NH_4 based on thermodynamic equilibrium; this is in contrast to a simple water-uptake curve based on only ammonium sulfate, as in most studies. Note that even though the SO_4 burden is predicted to decrease after 2050 as SO_2 emissions decrease, the total inorganic aerosol burden is still predicted to increase due to increased emissions of NO_x and NH_3 , which contribute to increased aerosol NO_3 and NH_4 burdens.

Comparison of model predicted sulfate concentrations with observations is provided by *Koch et al.* [1999], which use the same sulfate model and GCM as this study. The model predicts surface concentrations of sulfate well, particularly in North America where both magnitude and seasonality are reproduced well. Predicted sulfate concentrations in Europe are too high during summer and too low during winter. Discrepancy is likely caused by the lack for heterogeneous oxidation in the model. On the basis of very sparse data, the predicted sulfate concentrations are about 50% too high in the free troposphere of polluted regions. *Adams et al.* [1999] provide extensive comparison of modeled ammonium concentrations to observations. For aerosol ammonium, modeled concentrations are generally within a factor of 2 of observations. Predicted ammonium concentrations tend to be too

Table 6: Predicted Global Aerosol Burdens (Tg)

Aerosol	Preindustrial	2000	2025	2050	2075	2100
<i>Carbonaceous</i>						
BC	0.01	0.15	0.20	0.25	0.31	0.41
POA	0.07	0.62	0.82	1.0	1.3	1.7
<i>Inorganic</i>						
SO ₄ ²⁻	0.75	2.2	3.3	3.3	2.3	2.0
NH ₄ ⁺	0.11	0.52	0.78	0.89	0.94	1.0
NO ₃ ⁻	0.10	0.19	0.35	0.58	1.2	1.6
H ₂ O	2.7	7.1	9.7	10	10	12

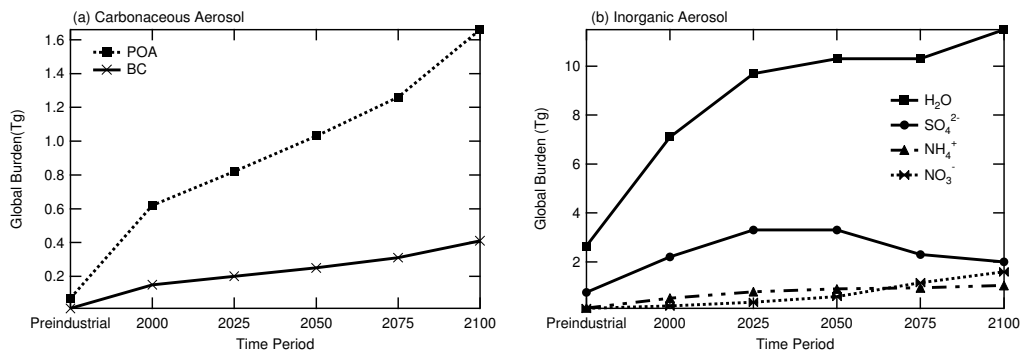


Figure 3: Estimates of global burden for (a) carbonaceous and (b) inorganic aerosols.

high compared with Eulerian Model Evaluation Field Study (EMEF5) data, which include measurements at approximately 130 sites spread throughout eastern North America [McNaughton *et al.*, 1996]. Chung and Seinfeld [2002] indicate that model predicted BC and OC concentrations are usually within an order of magnitude of observations. The emission rates of BC and OC used here are a factor of 2 lower than those of Chung and Seinfeld [2002]; therefore, the current model predictions are still within an order of magnitude of observations. Unfortunately, constraining the model predictions of global aerosol distribution is difficult due to lack of long term data. Subgrid variability in measured concentrations also hinders comparison with observations.

3.2 Radiative Effects of Black Carbon in the Atmosphere

Of all particulate species, black carbon exerts the most complex effect on climate. Like all aerosols, BC scatters a portion of the direct solar beam back to space, which leads to a reduction in solar radiation reaching the surface of the Earth. This reduction is manifest as an increase in solar radiation reflected back to space at the top of the atmosphere, that is, a *negative* radiative forcing (cooling). A portion of the incoming solar radiation is absorbed by BC-containing particles in the air. This absorption leads to a further reduction in solar radiation reaching the surface. At the surface, the result of this absorption is cooling because solar radiation that would otherwise reach the surface is prevented from doing so. However, the absorption of radiation by BC-containing particles leads to a heating in the atmosphere itself. Thus, absorption by BC leads to a negative radiative forcing at the surface and a positive radiative forcing in the atmosphere. Finally, the BC-containing aerosol absorbs radiation from the diffuse upward beam of scattered radiation. This reduces the solar radiation that is reflected back to space, leading to a positive radiative forcing at the top of the atmosphere. This effect is particularly accentuated when BC aerosol lies above clouds.

Top-of-atmosphere (TOA) forcing for BC is the sum of the negative forcing at the surface due to scattering of incoming radiation and the positive forcing from absorption of upward diffuse radiation. Note that the absorption of incoming solar radiation by BC does not contribute to TOA forcing because it adds heat to the atmosphere but reduces solar heating at the surface by the same amount. The net effect of BC is to add heat to the atmosphere and decrease radiative heating of the surface. The TOA radiative forcing for BC is the sum of the surface (negative) and atmospheric (positive) forcing.

Considering the other aerosol species (sulfates, nitrates, organics), at the TOA, black carbon opposes the cooling effect of the other components, but at the surface all aerosol species, BC included, lead to a reduction in solar radiation. Thus, while the overall net TOA radiative forcing might be modest because of the cancellation of negative and positive effects, aerosol-induced changes in radiation at the surface can be substantial. It has been estimated that anthropogenic absorbing aerosols can reduce solar radiation over land areas of the Earth by 3 to 5 W m^{-2} . Reduction in solar radiation at the surface of this magnitude can affect the hydrological cycle, since about 70% of solar radiation absorbed at the surface is turned into latent heat flux of evaporation.

An indirect radiative effect of BC arises when deposition of BC-containing aerosols over snow-covered areas lowers the albedo of the surface. And then a further reduction in surface albedo results when the heating by absorbing BC in the snow leads to enhanced melting [*Hansen and Nazarenko, 2004; Jacobson, 2004*].

Table 7: Estimates of Anthropogenic Direct Radiative Forcing at TOA (W m^{-2})

Aerosol	Year				
	2000	2025	2050	2075	2100
<i>Individual Component</i>					
BC	+0.39	+0.54	+0.68	+0.85	+1.15
POA	-0.10	-0.14	-0.17	-0.21	-0.28
$\text{SO}_4^{2-}/\text{NH}_4^+/\text{NO}_3^-/\text{H}_2\text{O}$	-0.74	-1.31	-1.40	-1.25	-1.37
<i>Mixture</i>					
External	-0.44	-0.90	-0.89	-0.60	-0.49
Internal	-0.10	-0.41	-0.25	+0.17	+0.49
<i>BC contribution to Internal Mixture^a</i>					
	+0.75	+1.03	+1.31	+1.62	+2.13

^a BC contribution to forcing of the internal mixture is calculated as forcing of the internal mixture minus that of an external mixture of POA and $\text{SO}_4^{2-}/\text{NH}_4^+/\text{NO}_3^-/\text{H}_2\text{O}$.

Estimated present-day greenhouse gas radiative forcings [*IPCC*, 2001]:

CO_2 :	+1.46	CH_4 :	+0.48
N_2O :	+0.15	Halocarbons:	+0.34
Total:	+2.43		

3.3 Direct Radiative Forcing Estimates

Estimates of global mean direct forcing are summarized in Tables 7 and 8 and shown in Figure 4. For internally mixed aerosols, identifying the contribution of each component to the total radiative forcing is difficult because total radiative forcing is not a just sum of those due to individual components. For the purpose of estimating the maximum BC contribution to direct radiative forcing, we take the direct radiative forcing of BC in an internal mixture to be the difference in radiative forcing between that of the internal mixture of BC, POA, and $\text{SO}_4^{2-}/\text{NH}_4^+/\text{NO}_3^-/\text{H}_2\text{O}$ aerosols and that of an external mixture of POA and $\text{SO}_4^{2-}/\text{NH}_4^+/\text{NO}_3^-/\text{H}_2\text{O}$ aerosols. The magnitude of both TOA and surface forcing for each individual species scales linearly with predicted global burden (see Table 6 and Figure 3). Under the external mixture assumption, the forcing efficiencies at TOA are approximately $+2.8 \text{ W m}^{-2}$ per Tg

Table 8: Estimates of Anthropogenic Direct Radiative Forcing at the Surface (W m^{-2})

Aerosol	Year				
	2000	2025	2050	2075	2100
<i>Individual Component</i>					
BC	-0.63	-0.87	-1.09	-1.36	-1.82
POA	-0.15	-0.20	-0.26	-0.32	-0.43
$\text{SO}_4^{2-}/\text{NH}_4^+/\text{NO}_3^-/\text{H}_2\text{O}$	-0.70	-1.25	-1.34	-1.20	-1.31
<i>Mixture</i>					
External	-1.48	-2.32	-2.70	-2.88	-3.56
Internal	-1.74	-2.67	-3.14	-3.42	-4.24
<i>BC contribution to Internal Mixture^a</i>					
	-0.89	-1.22	-1.54	-1.90	2.50

^a BC contribution to forcing of the internal mixture is calculated as forcing of the internal mixture minus that of and external mixture of POA and $\text{SO}_4^{2-}/\text{NH}_4^+/\text{NO}_3^-/\text{H}_2\text{O}$.

of anthropogenic BC, -0.18 W m^{-2} per Tg of anthropogenic POA, and -0.12 W m^{-2} per Tg of anthropogenic $\text{SO}_4^{2-}/\text{NH}_4^+/\text{NO}_3^-/\text{H}_2\text{O}$ aerosol, in agreement with forcing efficiencies determined by *Chung and Seinfeld* [2002]. At the surface, the forcing efficiencies are -4.5 W m^{-2} per Tg of anthropogenic BC, -0.17 W m^{-2} per Tg of anthropogenic POA, and -0.11 W m^{-2} per Tg of anthropogenic $\text{SO}_4^{2-}/\text{NH}_4^+/\text{NO}_3^-/\text{H}_2\text{O}$ aerosol. When internally mixed with other aerosols, the forcing efficiencies of BC increase to $+5.4$ and -6.4 at TOA and the surface, respectively.

Referring to Figure 4, the enhanced absorption by BC-containing particles in an internal mixture is clearly evident. The reason for the enhanced warming due to BC in an internal mixture is that, physically, POA and $\text{SO}_4^{2-}/\text{NH}_4^+/\text{NO}_3^-/\text{H}_2\text{O}$ in a sphere act as a lens that concentrates light to a focal volume. If black carbon is in that focal volume, absorption is enhanced over that if the black carbon particles remain separate from the other particles. [*Chýlek et al.*, 1995; *Fuller et al.*, 1999]. The exact degree of enhancement is a complicated function of particle size, mass mixing ratio, and geometrical distribution of the absorbing material within the particle. The enhancement calculated here most likely represents an upper estimate because of the use of the volume-averaged refractive index approximation

While cooling of $\text{SO}_4^{2-}/\text{NH}_4^+/\text{NO}_3^-/\text{H}_2\text{O}$ aerosol is predicted to level off after 2050 as SO_2 emission decreases, warming by BC and cooling by POA are predicted to

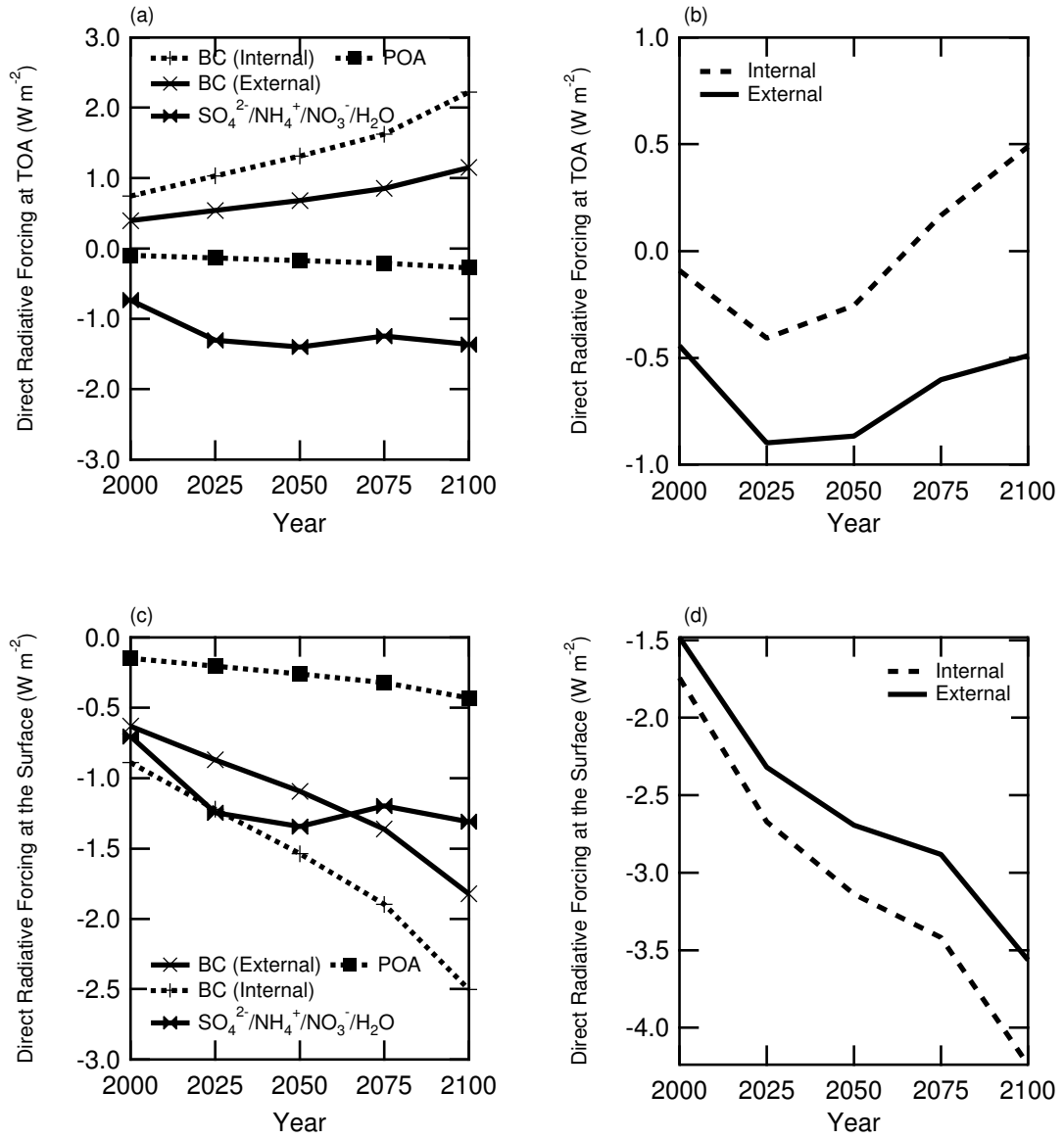


Figure 4: Estimates of global mean direct radiative forcings at TOA (top panel) and at the surface (bottom panel) and for individual aerosol (left panel) and aerosol mixtures (right panel).

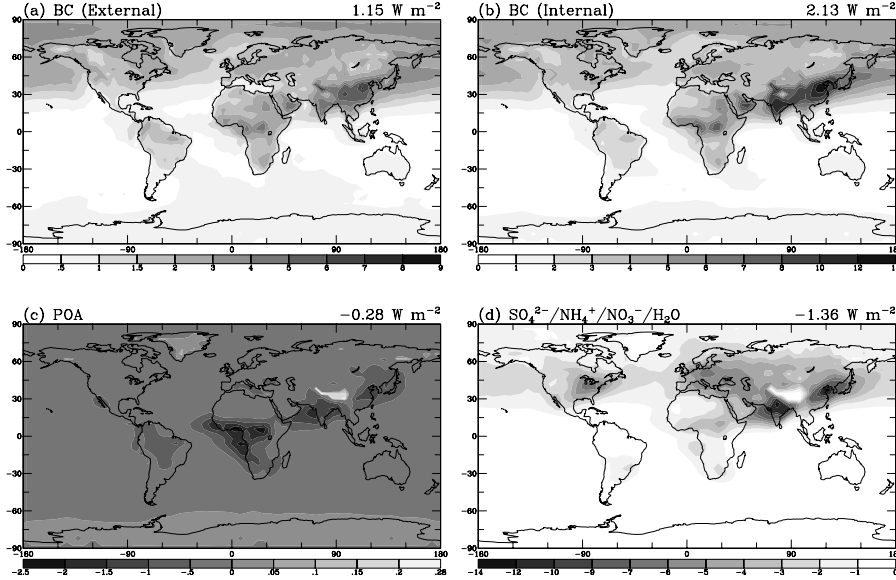


Figure 5: Predicted geographical distributions of predicted anthropogenic contribution to annual mean TOA direct radiative forcing (W m^{-2}) for the year 2100 for (a) Externally-mixed BC, (b) Internally-mixed BC, (c) POA, and (d) $\text{SO}_4^{2-}/\text{NH}_4^+/\text{NO}_3^-/\text{H}_2\text{O}$. The global averages are given on the upper right hand corner of each figure.

increase. For BC, anthropogenic direct radiative forcing at TOA is estimated to increase from $+0.4$ to $+1.1 \text{ W m}^{-2}$ from year 2000 to 2100 if BC is externally mixed with other aerosols. If BC is internally mixed with POA and $\text{SO}_4^{2-}/\text{NH}_4^+/\text{NO}_3^-/\text{H}_2\text{O}$ aerosol, then the increase is from $+0.7$ to $+2.1 \text{ W m}^{-2}$. Compared to BC, the magnitude of direct radiative forcing of anthropogenic POA is relatively small.

Under the external mixture assumption, by the year 2100, the combined effect of BC, POA, and $\text{SO}_4^{2-}/\text{NH}_4^+/\text{NO}_3^-/\text{H}_2\text{O}$ aerosols is that the net cooling at TOA is almost the same as the present day ($\sim 0.5 \text{ W m}^{-2}$); however, because of increased absorption of solar radiation by BC in the atmosphere, the cooling at the surface is more than doubled from -1.5 to -3.6 W m^{-2} . Under the internal mixture assumption, the effect of BC is even greater. In this case, the net effect of direct radiative forcing of anthropogenic BC, POA, and $\text{SO}_4^{2-}/\text{NH}_4^+/\text{NO}_3^-/\text{H}_2\text{O}$ at TOA is changed from net cooling of 0.1 W m^{-2} in 2000 to net warming of 0.5 W m^{-2} by 2100. Clearly, by 2100, based on the SRES A2 emissions scenario direct radiative forcing of BC is predicted to be as important as that of $\text{SO}_4^{2-}/\text{NH}_4^+/\text{NO}_3^-/\text{H}_2\text{O}$ aerosol.

The geographical distributions of the forcings are predicted to be similar for all time periods. To see the maximum forcing potential, the geographical distributions of predicted anthropogenic contribution to direct radiative forcing for the year 2100 at TOA and the surface are shown in Figures 5 and 6, respectively. As expected, the

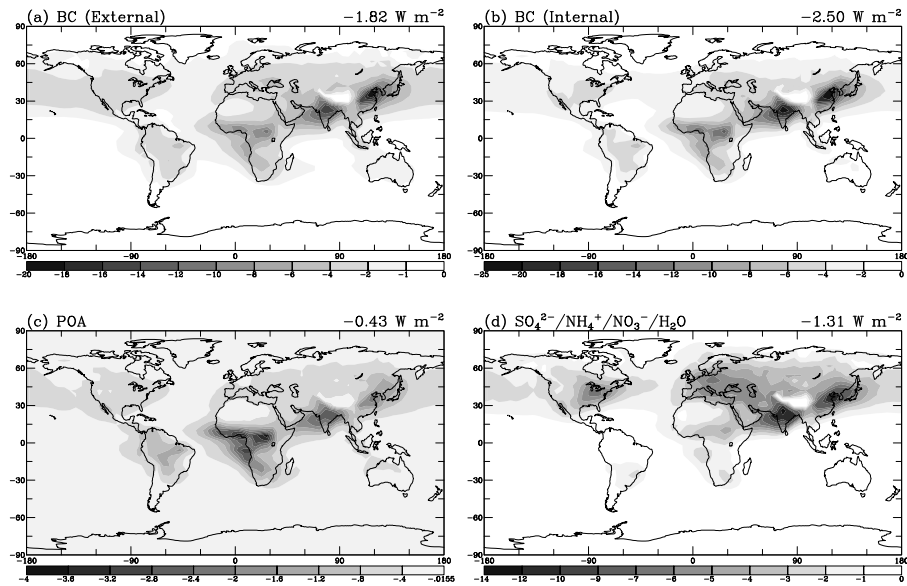


Figure 6: Predicted geographical distributions of predicted anthropogenic contribution to annual mean direct radiative forcing at the surface (W m^{-2}) for the year 2100 for (a) Externally-mixed BC, (b) Internally-mixed BC, (c) POA, and (d) $\text{SO}_4^{2-}/\text{NH}_4^+/\text{NO}_3^-/\text{H}_2\text{O}$. The global averages are given on the upper right corner of each figure.

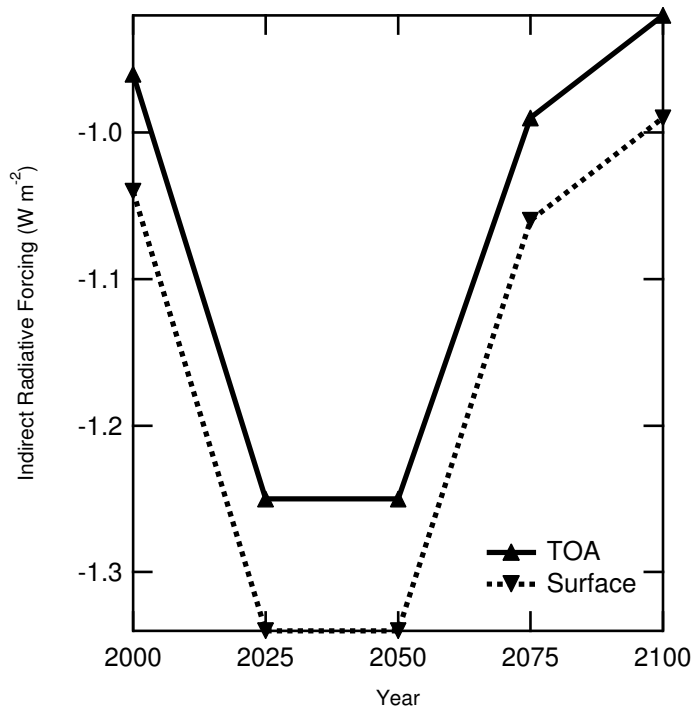


Figure 7: Predicted indirect radiative forcing of anthropogenic sulfate aerosol.

effect is predicted to be the greatest in continental regions where primary emissions are high, especially in eastern China, India, and Europe. For BC, the TOA forcing is also pronounced at high northern latitudes, where concentrations are not extremely large, but the high underlying surface albedo due to presence of ice and snow enhances the warming.

3.4 Indirect Radiative Forcing Estimates

Estimates of global mean indirect forcing attributable to sulfate aerosols are summarized in Table 9 and shown in Figure 7. As expected, indirect radiative forcing leads to net cooling at TOA as increased sulfate concentrations leads to increased cloud albedo, reflecting more solar radiation back to space. Note that the magnitude of the surface forcing is slightly greater than that at TOA because multiple reflections within the atmospheric column prevent even more solar radiation from reaching the surface. Indirect radiative forcing is predicted to be largest in the year 2025 as 2025 is the year of the greatest SO_2 emission. Predicted geographical distribution of the indirect forcing for 2025 is shown in Figure 8. Similar to direct radiative forcing, indirect radiative forcing is concentrated in polluted continental regions. Notice that by 2050, warming by direct radiative forcing of anthropogenic BC measured at TOA

Table 9: Predicted Indirect Radiative Forcing of Anthropogenic Sulfate Aerosol (W m^{-2})

	2000	2025	2050	2075	2100
TOA	-0.96	-1.25	-1.25	-0.99	-0.92
Surface	-1.04	-1.34	-1.34	-1.06	-0.99

is predicted to exceed the cooling by indirect radiative forcing of sulfate if BC is internally mixed with POA and $\text{SO}_4^{2-}/\text{NH}_4^+/\text{NO}_3^-/\text{H}_2\text{O}$. Under the external mixing assumption, warming by direct radiative forcing of anthropogenic BC predicted to exceed the cooling by indirect radiative forcing of sulfate by 2100. Based on these estimates, direct and indirect radiative forcing combined, sulfate is still more effective in cooling the atmosphere than BC is in warming the atmosphere.

3.5 Comparison with Other Studies

Because of imprecise knowledge of BC sources and uncertainties in simulation of aerosol removal mechanisms, any method of determining BC climate forcing based on global chemical transport models is rather uncertain. *Sato et al.* [2003] proposed an alternative empirical approach for estimating the BC amount, using sun photometer data in the longwave (red) portion of the spectrum. This approach is based on the fact that BC absorption exhibits a $1/\lambda$ spectral dependence over this entire wavelength range [*Bergstrom et al.*, 2002]. This makes it possible to distinguish BC from other absorbing aerosols, specifically organic carbon (OC) and soil dust, which have appreciable absorption only at $\lambda < 600$ nm [*d’Almeida et al.*, 1991]. *Sato et al.* [2003] employed the optical depths for aerosol absorption (σ_a) measured by AERONET photometers [*Holben et al.*, 2001; *Dubovik et al.*, 2002] at more than 100 sites around the world. They compared the aerosol absorption measured by AERONET with the aerosol absorption in the aerosol climatologies of *Koch* [2001] and *Chin et al.* [2002].

The aerosol compositions were treated by *Sato et al.* [2003] as if they were externally mixed in the aerosol climatologies and in the radiative forcing calculations. This assumption does not affect the resulting estimate for the BC climate forcing, because both the forcing and the AERONET-measured σ_a depend on the BC absorption, not the BC mass. However, it means that, because internally mixed BC is more effective at absorption [*Chýlek et al.*, 1995; *Jacobson*, 2001], the BC mass is somewhat less than obtained in the externally mixed approximation.

While BC is the aerosol species most responsible for absorption of solar radiation, OC [*Krivacsy et al.*, 2001] and soil dust [*d’Almeida et al.*, 1991] are also significant

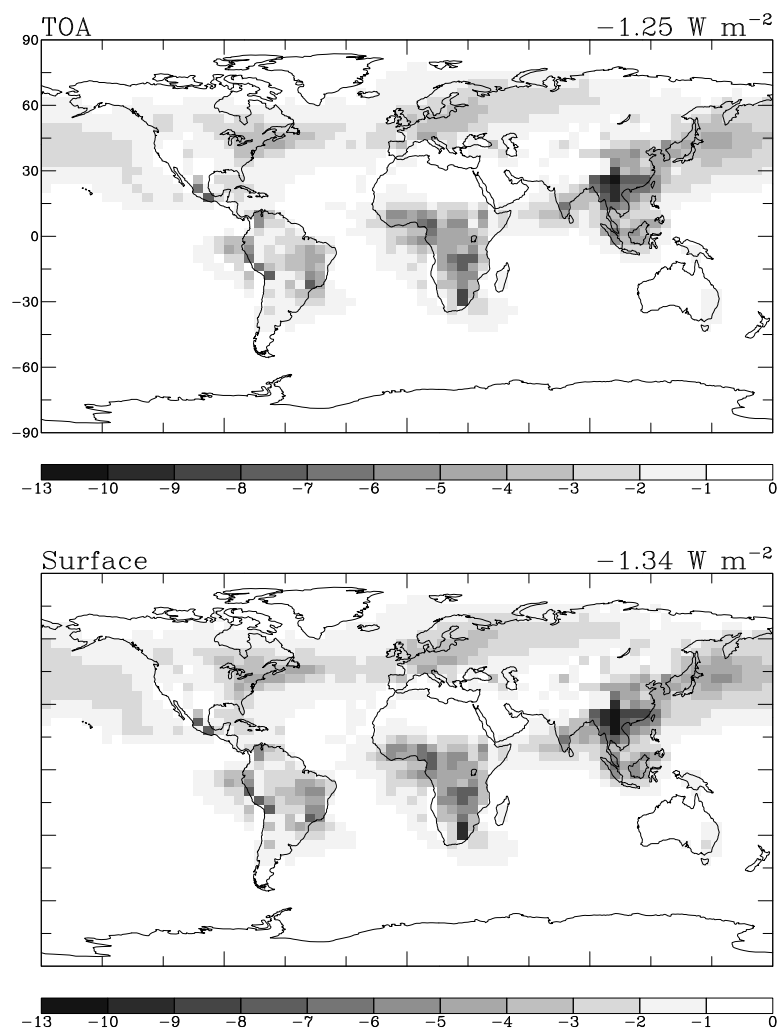


Figure 8: Geographical distribution of predicted indirect radiative forcing of anthropogenic sulfate aerosol for the year 2025.

absorbers, especially in the ultraviolet region. Therefore, *Sato et al.* [2003] accounted for the absorption of these latter species as well as possible, before attempting to infer BC absorption from AERONET observations.

Sato et al. [2003] conclude that there is more atmospheric absorption by BC aerosols than has generally been realized. This could not be the case if either the AERONET measurements are inaccurate, with excessively large absorption, or there is another strong absorber at the red wavelengths, in addition to BC. Aerosol absorption is summarized in the single scatter albedo, ω . At the AERONET sites, mostly continental, the mean value of ω decreases monotonically from 0.914 at 670 nm to 0.897 at 1020 nm.

If there is an unidentified material providing the absorption, the absorber would need to have properties similar to those of BC in the sense of providing comparable absorption at all three AERONET channels between 670 and 1020 nm. *Hansen et al.* [2000] show that aerosols and water vapor accurately reproduce atmospheric transmission data and *Kaufman et al.* [2002] use AERONET measurements to show that there is no significant non-aerosol absorption in spectral bands without gaseous absorption. *Hu man* [1996] and references cited therein, show that BC accounts for most of the aerosol absorption in continental regions.

Sato et al. [2003] estimate the current anthropogenic BC forcing as about 0.7 ± 0.2 W m^{-2} . The indicated uncertainty is a subjective 1σ estimate. This BC climate forcing is larger than the 0.3 W m^{-2} estimated by *IPCC* [2001], although *IPCC*'s estimate referred only to the fossil fuel component. The derived BC climate forcing is reasonably consistent with an estimate by *Jacobson* [2001] of about 0.5 W m^{-2} for the fossil fuel component. It is also consistent with the estimate $0.8 \pm 0.4 \text{ W m}^{-2}$ for the total BC forcing by *Hansen and Sato* [2001] who included indirect BC forcings such as reduced snow albedo. Finally, as noted earlier, *Chung and Seinfeld* [2002] estimated that present-day BC direct radiative forcing lies in a range between 0.51 W m^{-2} (100% external mixing) and 0.8 W m^{-2} (100% internal mixing). As seen, this range encompasses the 0.7 W m^{-2} BC forcing of *Sato et al.* [2003] based on AERONET data.

Sato et al. [2003] conclude that BC aerosols cause a larger climate forcing than has been assumed by *IPCC* [1996, 2001]. This large positive climate forcing has occurred in approximately the same regions of the globe as the negative direct and indirect climate forcings by reflective aerosols (sulfates, nitrates, and OC). *Sato et al.* [2003] suggest that this large positive BC forcing provides a partial explanation for why global warming has proceeded rapidly despite the fact that the estimated negative (direct plus indirect) forcing by reflective aerosols is almost as large as the positive forcing by long-lived greenhouse gases [*IPCC*, 2001; *Hansen and Sato*, 2001]. Another air pollutant, tropospheric ozone, contributes in a similar way to BC [*Hansen and Sato*, 2001].

Some have suggested that policy-makers should place at least as much emphasis on reducing BC aerosols (“soot”) as on reducing reflective aerosols. It has even been suggested that reducing BC aerosols may be the best strategy to slow global

warming [*Jacobson, 2002*]. Reduction of BC emissions could minimize the global warming bounce that will result from reductions in reflective aerosols. *Sato et al. [2003]* argue that

“first, actions to reduce BC will also reduce OC from the same sources, and the negative OC forcing counterbalances about half of the BC forcing. Second, some of the actions that reduce BC and OC require reducing the sulfur content of fuels, which will reduce the negative forcing by sulfate aerosols. Third, reduced aerosol amounts will tend to reduce the (negative) indirect aerosol forcing due to their effects on clouds. Fourth, the efficacy of the direct climate forcing by absorbing aerosols is less than that for the same forcing by CO₂ and other well-mixed greenhouse gases, i.e., it is less effective in producing warming of surface air temperature [*Hansen et al., 1997*]. For these reasons, the cooling effect of actions to reduce BC emissions will be small. Nevertheless, we agree that such actions are desirable not only to minimize the warming from expected reductions in reflective aerosols, but also to reduce regional climate impacts of BC aerosols and reduce human health and agricultural impacts of these aerosols.”

3.6 Efficacy of Climate Forcings

The efficacy of a climate forcing can be defined as the global mean temperature change produced by the forcing relative to the global mean temperature change produced by a CO₂ forcing of the same magnitude. Hansen introduced this effective forcing concept and terminology because it was realized that the climate effect of pollutants such as soot and ozone was complex, depending especially on their spatial distribution. CO₂ provides an apt basis for comparison, because the anthropogenic increase of atmospheric CO₂ is the largest anthropogenic climate forcing [*IPCC, 2001*]. Attempts to slow global warming must focus primarily on restricting CO₂ emissions. Therefore, in considering the merits of reducing other forcings, it is helpful to know their contributions to global warming relative to that of CO₂. Efficacies are computed based on a 100 year simulation (or longer) and therefore include all climate feedbacks that operate on that time scale.

The climate forcing by CO₂ in the present GISS Model III is at the high end of the range estimated by IPCC [*Ramaswamy et al., 2001*]. Specifically, doubled CO₂ in the current model, from the 1880 value of 291 ppm to 582 ppm, yields forcing = 4.12 W m⁻² ($F_0 = 3.78 \text{ W m}^{-2}$, $\delta T_0 = 0.22\text{K}$, $\lambda = 2/3 \text{ K per W m}^{-2}$). IPCC [*Ramaswamy et al., 2001*] estimates forcing for doubled CO₂ to be in the range 3.5-4.1 W m⁻². If the actual CO₂ forcing is at the low end of this range, the GISS CO₂ forcing and simulated climate response will be reduced as much as 15%. The efficacies are not affected substantially by the uncertainty in the CO₂ forcing, because the efficacies are defined relative to a CO₂ forcing of the same magnitude, not relative to a given

CO₂ amount.

Hansen et al. [2005] report a 120-year coupled model simulation with all well-mixed GHGs (CO₂, CH₄, N₂O and CFCs) increased from 1880 to 2000 values that yields $\Delta T_S = 1.21 \pm 0.02^\circ\text{C}$ for years 81-120, where the indicated uncertainty is the standard deviation of the five ensemble members. $\Delta T_S = 1.21^\circ\text{C}$ corresponds to an efficacy $E_a \sim 110\%$. This result implies, because more than half of the GHG forcing for that period is from CO₂, that the efficacy of the non-CO₂ gases is substantially higher than 100%.

Absorbing aerosols, like BC, represent the prime climate forcing agent for which the magnitude of radiative forcing is not necessarily a good indicator of the climate response, that is, the efficacy can be much different from unity. *Hansen et al.* [2005] find that BC aerosols from biomass burning have a calculated efficacy of 59%, while fossil fuel BC has an efficacy of 79%. Predicted global warming is close to 1°C when all the BC is assumed to be in the planetary boundary layer and 0.3°C when the BC is all in the free troposphere. Thus the climate efficacy of BC decreases markedly as more of the BC is found in the upper troposphere. The large change in efficacy with the altitude of BC is due, in part, to the reduction in cloud cover that results from heating of the layer by BC. Heating of the layer containing the aerosols lowers cloud cover in that layer, but that heating also inhibits convection from the layer below and, in so doing, leads to an increase in cloud cover in the layer below. *Roberts and Jones* [2004] studied the climate sensitivity to fossil fuel black carbon using the Hadley Centre GCM. They obtained a climate sensitivity of 0.56°C per W m^{-2} for BC versus 0.91°C per W m^{-2} for CO₂. Thus, their fossil fuel BC efficacy is about 62%, as compared with the 79% obtained by *Hansen et al.* [2005]. Because BC climate efficacy is so sensitive to the altitude distribution of BC, more work will be needed to better constrain these efficacies.

4 Discussion

Under the SRES emission scenario A2, emissions of BC and POA are expected to increase continuously from 2000 to 2100 while emissions of SO₂ are expected to decline after 2050. Therefore, the BC contribution to total direct radiative forcing of aerosols will become more important after 2050. Under the internal mixture assumption, by 2100, direct radiative forcing of anthropogenic BC at TOA is predicted to be +2.1 W m^{-2} , which almost cancels the -2.6 W m^{-2} due to direct radiative forcings of POA and SO₄²⁻/NH₄⁺/NO₃⁻/H₂O aerosol and indirect radiative forcing of sulfate combined. Given the large uncertainties of indirect forcing estimates, indirect forcing of sulfate aerosol could be overestimated, suggesting that, if emissions are unchecked and BC is internally mixed with other aerosols, BC can potentially cancel out the cooling effect of other aerosols after 2050.

According to *Bond et al.* [2004], BC emissions from contained combustion (i.e. fossil fuel and biofuel combustion) in North America is currently 382 Gg yr^{-1} . The

total population in North America is 428 million, of which about 35 million live in California. Using population as a proxy, then current BC emissions from California due to contained combustion are approximately 31 Gg yr^{-1} , which is approximately 0.4% of the present-day estimated global emission of anthropogenic BC. Assuming that radiative forcing scales linearly with emission rate, then the State of California is responsible currently for approximately 0.4% of the global mean direct radiative forcing attributable to BC. Under the external mixture assumption, fossil fuel and biofuel BC currently emitted in California is predicted to contribute to TOA direct radiative forcing an amount equal to $+0.001 \text{ W m}^{-2}$, with this forcing increasing to $+0.005 \text{ W m}^{-2}$ by 2100. If BC is internally mixed with POA and $\text{SO}_4^{2-}/\text{NH}_4^+/\text{NO}_3^-/\text{H}_2\text{O}$, then the contribution from California increases to $+0.002$ and $+0.008 \text{ W m}^{-2}$ for 2000 and 2100, respectively.

Determining California's contribution to CO_2 radiative forcing is difficult because, unlike aerosols, CO_2 has a long atmospheric lifetime such that the present-day forcing is the result of accumulation of CO_2 emissions over several decades. We get an estimate of California's contribution to TOA direct radiative forcing of CO_2 using two simplifying assumptions: 1) the present-day United State's contribution to TOA direct radiative forcing of CO_2 scales linearly with present-day CO_2 emissions; and 2) within the U.S., each state's contribution to CO_2 forcing is proportional to its population. These assumptions ignore CO_2 emissions prior to the present day and natural emissions of CO_2 , which is negligible relative to anthropogenic emissions for the present day. From the 1995 emissions inventory of EDGAR 3 [Olivier and Berdowski, 2001], the emissions of CO_2 are approximately $2.7 \times 10^4 \text{ Tg yr}^{-1}$ and $5.6 \times 10^3 \text{ Tg yr}^{-1}$ globally and in the U.S., respectively. According the U.S. 2000 census, approximately 12% of the U.S. population live in California. Based on these emissions estimates and population data, California's contribution to TOA direct radiative forcing of CO_2 for the year 2000 is approximately $1.46 \times 0.12 \times 5.6 \times 10^3 / 2.7 \times 10^4 = 0.04 \text{ W m}^{-2}$, which is about 20 to 40 times as much as California's contribution to TOA direct radiative forcing of BC.

5 Summary and Conclusions

Using Scenario A2 of the Intergovernmental Panel on Climate Change Special Report on Emission Scenarios, direct radiative forcings of anthropogenic BC, POA, and $\text{SO}_4^{2-}/\text{NH}_4^+/\text{NO}_3^-/\text{H}_2\text{O}$ aerosol and indirect forcing forcing of anthropogenic sulfate aerosol at top of the atmosphere and at the surface have been estimated online in the Goddard Institute for Spaces Studies General Circulation Model II-Prime for the years 2000, 2025, 2050, 2075, and 2100. As SO_2 emissions slowly decline, anthropogenic BC is predicted to become an increasingly important contributor to total direct radiative forcing over the next one hundred years if BC emissions stay uncurtailed. The effect of BC is especially significant radiatively if BC is assumed to be internally mixed with POA and $\text{SO}_4^{2-}/\text{NH}_4^+/\text{NO}_3^-/\text{H}_2\text{O}$ aerosol. By 2075, the con-

tribution of BC is predicted to be sufficiently large that warming by BC dominates cooling by POA and $\text{SO}_4^{2-}/\text{NH}_4^+/\text{NO}_3^-/\text{H}_2\text{O}$ such that a net warming is predicted for the internal mixture of BC, POA, and $\text{SO}_4^{2-}/\text{NH}_4^+/\text{NO}_3^-/\text{H}_2\text{O}$ aerosols. Even when cooling by indirect radiative forcing of sulfate is considered at the estimated levels (Figure 7), which are highly uncertain, warming due to internally-mixed BC can potentially cancel the combined coolings of other aerosols. Based on population, biofuel and fossil fuel BC emissions from California are estimated to contribute approximately 0.4% of the global mean direct radiative forcing of anthropogenic BC.

6 Recommendations

The motivation of the present study is to obtain an estimate of the climatic effect of black carbon emissions from the State of California. Given such an estimate, one can then proceed to compare the relative climatic effects of CO_2 and black carbon emitted by California. This will provide state legislators with information needed when considering CO_2 and BC abatement policies motivated by future climate effects.

As in all studies of global climate effects of gases and aerosols, the most important input is the emissions themselves. In the current study, we have estimated present-day BC emissions from California by scaling the recent BC inventory of *Bond et al.* [2004] to California on the basis of population. The extent to which this estimate is accurate is unknown. Therefore, our first recommendation is that the State of California prepare a current emissions inventory for black carbon particulate matter (We understand that this is already underway.) Because of the role of BC particulate matter in both climate and human health effects, this endeavor is highly recommended.

A next step in this overall project is to study climatic effects on California of greenhouse gas and aerosol radiative forcing over the next century. This would involve evaluating different greenhouse gas and aerosol emission scenarios, with special attention to the relative emissions of CO_2 and black carbon. Climatic effects would include surface temperature and precipitation rates and patterns. Such a study would require a GCM having as fine a spatial resolution as possible, so as to be able to resolve climatic variations on a spatial scale of California. Currently, the finest GCM resolutions are the order of $2^\circ \times 2.5^\circ$ latitude by longitude, e.g., the GISS Model E [*Schmidt et al.*, 2005]. The results of the current study can serve as input information to such a climate study.

In this report we have argued that indirect climatic effects of BC on cloud formation are small owing to the fact that BC must become coated by soluble aerosol material before being able to function as a CCN, and that, on a mass basis, soluble sulfate and organic carbon substantially exceed that of BC globally. This argument is supported by the very recent work of *Hansen et al.* [2005], which estimates that about 6% of global indirect aerosol forcing can be attributed to BC. Nevertheless, current estimates of indirect forcing, on the whole, remain quite uncertain; even more uncertain are the contributions to indirect aerosol forcing by individual aerosol

species. Such contributions are even more difficult to unravel because aerosols in the atmosphere generally exist as internal mixtures. Research continues to be carried out actively worldwide aimed at trying to understand and unravel indirect aerosol effects. Still, the extent to which aerosol indirect forcing (by sulfates and organic aerosols predominantly) will affect the hydrological cycle in California should be examined using the best current aerosol/cloud parameterizations available for GCMs.

References

- Ackerman, A. S., O. B. Toon, D. E. Stevens, A. J. Heymsfield, V. Ramanathan, and E. J. Welton, Reduction of tropical cloudiness by soot, *Science*, *288*, 1042–1047, 2000.
- Ackerman, A. S., O. B. Toon, D. E. Stevens, and J. A. Coakley, Jr, Enhancement of cloud cover and suppression of nocturnal drizzle in stratocumulus polluted by haze, *Geophys. Res. Lett.*, *30*(7), 1381, doi:10.1029/2002GL016634, 2003.
- Adams, P. J., J. H. Seinfeld, and D. M. Koch, Global concentrations of tropospheric sulfate, nitrate, and ammonium aerosol simulated in a general circulation model, *J. Geophys. Res.*, *104*, 13,791–13,823, 1999.
- Adams, P. J., J. H. Seinfeld, D. M. Koch, L. Mickley, and D. Jacob, General circulation model assessment of direct radiative forcing by sulfate-nitrate-ammonium-water inorganic aerosol system, *J. Geophys. Res.*, *106*(D1), 1097–1111, 2001.
- Albrecht, B. A., Aerosols, cloud microphysics, and fractional cloudiness, *Science*, *245*(4923), 1227–1230, 1989.
- Bergstrom, R. W., P. B. Russell, and P. Hignett, Wavelength dependence of the absorption of black carbon particles: predictions and results from the TARFOX experiment and implications for the aerosol single scattering albedo, *J. Atmos. Sci.*, *59*(3), 567–577, 2002.
- Bigg, E. K., Discrepancy between observation and prediction of concentrations of cloud condensation nuclei, *Atmos. Res.*, *20*, 81–86, 1986.
- Boers, R., and R. M. Mitchell, Absorption feedback in stratocumulus clouds : Influence on cloud-top albedo, *Tellus*, *46A*(3), 229–241, 1994.
- Bohren, C. F., and D. R. Hu man, *Absorption and Scattering of Light by Small Particles*, John Wiley & Sons, Inc., New York, NY, 1983.
- Bond, T. C., and R. W. Bergstrom, Toward resolution on the optics of light-absorbing carbon, in *AGU Fall Meeting*, San Francisco, USA, 2004.
- Bond, T. C., D. G. Streets, K. F. Yarber, S. M. Nelson, J. Woo, and Z. Klimont, A technology-based global inventory of black and organic carbon emissions from combustion, *J. Geophys. Res.*, *109*(D14), D14203, doi:10.1029/2003JD003697, 2004.
- Boucher, O., and T. L. Anderson, General circulation model assessment of the sensitivity of direct radiative forcing by sulfate aerosols to size and chemistry, *J. Geophys. Res.*, *100*, 26,117–26,134, 1995.

- Boucher, O., and U. Lohmann, The sulfate-CCN-cloud albedo effect: A sensitivity study with two general circulation models, *Tellus*, *47B*, 281–300, 1995.
- Bouwman, A. F., D. S. Lee, W. A. H. Asman, F. J. Dentener, K. W. van der Hoek, and J. G. J. Olivier, A global high resolution emission inventory for ammonia, *Global Biogeochem. Cycles*, *11*, 561–587, 1997.
- Brenguier, J.-L., and Y. Fouquart, Introduction to EUCREX-98 mission 206, *Atmos. Res.*, *55*, 3–14, 2000.
- Brenguier, J.-L., H. Pawlowska, L. Schüller, R. Preusker, J. Fischer, and Y. Fouquart, Radiative properties of boundary layer clouds: Droplet effective radius versus number concentrations, *J. Atmos. Sci.*, *57*, 803–821, 2000.
- Bréon, F.-M., D. Tanre, and S. Generoso, Aerosol effect on cloud droplet size monitored from satellite, *Science*, *295*, 831–838, 2002.
- California Air Resources Board, *Identification of particulate matter species profiles, ARB Speciation Manual, Second Edition, Volume 2*, Sacramento, CA, 1999.
- Cantrell, W., G. Shaw, C. Leck, and H. Cachier, Relationships between cloud condensation nuclei spectra and aerosol particles on a south-north transect of the Indian Ocean, *J. Geophys. Res.*, *105*, 153,131–15,320, 2000.
- Cantrell, W., G. Shaw, G. R. Cass, Z. Chowdhury, L. S. Hughes, K. A. Prather, S. A. Guazzotti, and K. R. Coe, Closure between aerosol particles and cloud condensation nuclei at Kaashidhoo Climate Observatory, *J. Geophys. Res.*, *106*, 28,711–28,718, 2001.
- Charlson, R. H., J. H. Seinfeld, A. Nenes, M. Kulmala, A. Laaksonen, and M. C. Facchini, Reshaping the theory of cloud formation, *Science*, *292*, 2025–2026, 2001.
- Charlson, R. J., J. Langner, H. Rodhe, C. B. Leovy, and S. G. Warren, Perturbation of the Northern Hemisphere radiative balance by backscattering from anthropogenic sulfate aerosols, *Tellus*, *43AB*, 152–163, 1991.
- Chin, M., P. Ginoux, S. Kinne, O. Torres, B. N. Holben, B. N. Duncan, R. V. Martin, J. A. Logan, A. Higurashi, and T. Nakajima, Tropospheric aerosol optical thickness from the GOCART model and comparisons with satellite and sun photometer measurements, *J. Atmos. Sci.*, *59*(3), 461–483, 2002.
- Chow, J. C., and J. G. Watson, *Imperial Valley/Mexicali Cross Border PM₁₀ Transport Study*, Desert Research Institute, Reno, NV; DRI Document No. 8623.2D1, 1995.

- Chuang, C. C., J. E. Penner, K. E. Taylor, A. S. Grossman, and J. J. Walton, An assessment of the radiative effects of anthropogenic sulfate, *J. Geophys. Res.*, *102*(D3), 3761–3778, 1997.
- Chuang, P. Y., D. R. Collins, H. Pawlowska, J. R. Snider, H. H. Jonsson, J.-L. Brenguier, R. C. Flagan, and J. H. Seinfeld, CCN measurements during ACE-2 and their relationship to cloud microphysical properties, *Tellus*, *52B*, 843–867, 2000.
- Chung, S. H., and J. H. Seinfeld, Global distribution and climate forcing of carbonaceous aerosols, *J. Geophys. Res.*, *107*(D19), 4407, doi:10.1029/2001JD001397, 2002.
- Chýlek, P., G. Videen, D. Ngo, R. G. Pinnick, and J. D. Klett, Effect of black carbon on the optical properties and climate forcing of sulfate aerosols, *J. Geophys. Res.*, *100*(D8), 16,325–16,332, 1995.
- Coakley, J. A., and C. D. Walsh, Limits to the aerosol indirect radiative effect derived from observations of ship tracks, *J. Atmos. Sci.*, *59*, 668–680, 2002.
- Conant, W. C., A. Nenes, and J. H. Seinfeld, Black carbon radiative heating effects on cloud microphysics and implications for the aerosol indirect effect: 1. Extended köhler theory, *J. Geophys. Res.*, *107*(D21), 4604, doi:10.1029/2002JD002094, 2002.
- Conant, W. C., T. M. VanReken, T. A. Rissman, V. Varutbangkul, H. H. Jonsson, A. Nenes, J. L. Jimenez, A. Delia, R. Bahreini, G. Roberts, R. C. Flagan, and J. H. Seinfeld, Aerosol-cloud drop concentrations closure in warm cumulus, *J. Geophys. Res.*, *109*, D13204, doi:10.1029/2003JD004324, 2004.
- Cooke, W. F., and J. J. N. Wilson, A global black carbon aerosol model, *J. Geophys. Res.*, *101*(D14), 19,395–19,409, 1996.
- Cooke, W. F. C., C. Liou, H. Cachier, and J. Feichter, Construction of a $1^\circ \times 1^\circ$ fuel emission data set for carbonaceous aerosol and implementation and radiative impact in the ECHAM4 model, *J. Geophys. Res.*, *104*(D18), 22,137–22,162, 1999.
- d’Almeida, G. A., P. Koepke, and E. P. Shettle, *Atmospheric Aerosol: Global Climatology and Radiative Characteristics*, A. Deepak Publishing, Hampton, VA, 1991.
- Del Genio, A. D., and Y. Yao, Efficient cumulus parameterization for long-term climate studies: The GISS scheme, in *The Representation of Cumulus Convection in Numerical Models Monogr. 46*, edited by K. E. Emanuel and D. J. Raymond, pp. 181–184, American Meteorol. Soc., Boston, Mass., 1993.
- Del Genio, A. D., M.-S. Yao, W. Kavari, and K. K.-W. Lo, A prognostic cloud water parameterization for global climate models, *J. Clim.*, *9*, 270–304, 1996.

- Dubovik, O., B. N. Holben, T. F. Eck, A. Smirnov, Y. J. Kaufman, M. D. King, D. Tanre, and I. Slutsker, Variability of absorption and optical properties of key aerosol types observed in worldwide locations, *J. Atmos. Sci.*, *59*, 590–608, 2002.
- Facchini, M. C., M. Mircea, S. Fuzzi, and R. J. Charlson, Cloud albedo enhancement by surface-active organic solutes in growing droplets, *Nature*, *401*, 257–259, 1999.
- Feichter, J., U. Lohmann, and I. Schult, The atmospheric sulfur cycle in ECHAM-4 and its impact on the shortwave radiation, *Clim. Dynam.*, *13*(4), 235–246, 1997.
- Feingold, G., and P. Y. Chuang, Analysis of the influence of film-forming compounds on droplet growth: Implications for cloud microphysical processes and climate, *J. Atmos. Sci.*, *59*, 2006–2018, 2002.
- Ferek, R. J., R. T. Garrett, P. V. Hobbs, S. Strader, D. Johnson, J. P. Taylor, K. Nielsen, A. S. Ackerman, Y. Kogan, Q. Liu, B. A. Albrecht, and D. Babb, Drizzle suppression in ship tracks, *J. Atmos. Sci.*, *57*(16), 2707–2728, 2000.
- Fitzgerald, J. W., Approximation formulas for the equilibrium size of an aerosol as a function of its dry size and composition and the ambient relative humidity, *J. Appl. Meteorol.*, *14*, 1044–1049, 1975.
- Forster, P., M. Blackburn, R. Glover, and K. Shine, An examination of climate sensitivity for idealised climate change experiments in an intermediate general circulation model, *Clim. Dynam.*, *16*(10-11), 833–849, 2000.
- Fuller, K. A., W. C. Malm, and S. M. Kreidenweis, Effects of mixing on extinction by carbonaceous particles, *J. Geophys. Res.*, *104*(D13), 15,941–15,954, 1999.
- Gerber, H., Microphysics of marine stratocumulus clouds with two drizzle modes, *J. Atmos. Sci.*, *53*, 1649–1662, 1996.
- Ghan, S. J., R. C. Easter, E. G. Chapman, H. Abdul-Razzak, Y. Zhang, L. R. Leung, N. S. Laulainen, R. D. Saylor, and R. A. Zaveri, A physically based estimate of radiative forcing by anthropogenic sulfate aerosol, *J. Geophys. Res.*, *106*(D6), 5279–5293, 2001.
- Grégoire, J.-M., K. Tansey, and J. Silva, The GBA2000 initiative: Developing a global burned area database from SPOT-VEGETATION imagery, *Int. J. Remote Sens.*, *24*(6), 1369–1376, 2003.
- Gultepe, I., and G. A. Isaac, Scale effects on averaging of cloud droplet and aerosol number concentrations: Observations and models, *J. Clim.*, *12*, 1268–1279, 1999.
- Han, Q., W. B. Rossow, J. Zeng, and R. Welch, Three different behaviors of liquid water path of water clouds in aerosol-cloud interactions, *J. Atmos. Sci.*, *59*(3), 726–735, 2002.

- Hansen, J., and L. Nazarenko, Soot climate forcing via snow and ice albedos, *Proc. Natl. Acad. Sci.*, *101*(2), 123–428, doi:10.1073/pnas.2237157100, 2004.
- Hansen, J., and M. Sato, Trends of measured climate forcing agents, *Proc. Natl. Acad. Sci. USA*, *98*, 14,778–14,783, 2001.
- Hansen, J., G. Russell, D. Rind, P. Stone, A. Lacis, S. Lebedev, R. Ruedy, and L. Travis, Efficient three-dimensional global models for climate studies: Model I and II, *Mon. Weather Rev.*, *111*, 609–662, 1983.
- Hansen, J., A. Lacis, G. Russell, P. Stone, I. Fung, R. Ruedy, and J. Lerner, Climate sensitivity: Analysis of feedback mechanisms, in *Climate Processes and Climate Sensitivity, Geophys. Monogr. Ser., Vol. 29*, edited by J. E. Hansen and T. Takahashi, pp. 130–163, American Geophysical Union, Washington, D.C., 1984.
- Hansen, J., M. Sato, and R. Ruedy, Long-term changes of the diurnal temperature cycle: implications about mechanisms of global climate change, *Atmos. Res.*, *37*, 175–209, 1995.
- Hansen, J., M. Sato, and R. Ruedy, Radiative forcing and climate response, *J. Geophys. Res.*, *102*(D6), 6831–6864, 1997.
- Hansen, J., R. Ruedy, A. Lacis, M. Sato, L. Nazarenko, N. Tausnev, I. Tegen, and D. Koch, Climate modeling in the global warming debate, in *General Circulation Model Development*, edited by D. A. Randall, pp. 127–164, Academic Press, New York, 2000.
- Hansen, J. et al., Efficacy of climate forcings, *J. Geophys. Res.*, submitted, 2005.
- Harshvardhan, S. E. Schwartz, C. M. Benkovitz, and G. Guo, Aerosol influences on cloud microphysics examined by satellite measurements and chemical transport modeling, *J. Atmos. Sci.*, *59*(3), 714–725, 2002.
- Hartke, G. J., and D. Rind, Improved surface and boundary layer models for the Goddard Institute for Space Studies general circulation model, *J. Geophys. Res.*, *102*, 16,407–16,422, 1997.
- Haywood, J. M., D. L. Roberts, A. Slingo, J. M. Edwards, and K. P. Shine, General circulation model calculations of the direct radiative forcing by anthropogenic sulfate and fossil-fuel soot aerosol, *J. Clim.*, *10*, 1562–1577, 1997.
- Holben, B. N., D. Tanre, A. Smirnov, T. F. Eck, I. Slutsker, N. Abuhassan, W. W. Newcomb, J. S. S. JS, B. Chatenet, F. Lavenu, Y. J. Kaufman, J. V. Castle, A. Setzer, B. Markham, D. Clark, R. Frouin, R. Halthore, A. K. A., N. T. O’Neill, C. P. C, R. T. Pinker, K. V. K, and G. Zibordi, An emerging ground-based aerosol climatology: Aerosol optical depth from AERONET, *J. Geophys. Res.*, *106*(D11), 12,067–12,097, 2001.

- Houghton, J. T., L. G. Meira, B. A. Callander, N. H. A. Kattenberg, and K. Maskell (Eds.), *Intergovernmental Panel on Climate Change, Climate Change 1995: The Science of Climate Change*, Cambridge Univ. Press, Cambridge, U.K., 1996.
- Houghton, J. T., Y. Ding, D. J. Griggs, M. Noguer, P. J. van der Linden, D. Xiaosu, K. Maskell, and C. A. Johnson (Eds.), *Intergovernmental Panel on Climate Change, Climate Change 2001: The Scientific Basis*, Cambridge Univ. Press, Cambridge, U.K., 2001.
- Hudson, J., and X. Da, Volatility and size of cloud condensation nuclei, *J. Geophys. Res.*, *101*, 4435–4442, 1996.
- Hu man, H. D., Comparison of light absorption coefficient and carbon measures for remote aerosols: An independent analysis of data from the IMPROVE network-1., *Atmos. Environ.*, *30*(1), 73–83, 1996.
- Jacobson, M. Z., A physically-based treatment of elemental carbon optics: Implication for global direct forcing of aerosols, *Geophys. Res. Lett.*, *27*(2), 217–220, 2000.
- Jacobson, M. Z., Strong radiative heating due to the mixing state of black carbon in atmospheric aerosols, *Nature*, *409*(6821), 695–697, 2001.
- Jacobson, M. Z., Control of fossil-fuel particulate black carbon and organic matter, possibly the most effective method of slowing global warming, *J. Geophys. Res.*, *107*(D19), 4410, doi:10.1029/2001JD001376, 2002.
- Jacobson, M. Z., Climate response of fossil fuel and biofuel soot, accounting for soot’s feedback to snow and sea ice albedo and emissivity, *J. Geophys. Res.*, *109*, D21201, doi:10.1029/2004JD004945, 2004.
- Joshi, M., K. Shine, M. Ponater, N. Stuber, R. Sausen, and L. Li, A comparison of climate response to different radiative forcings in three general circulation models: toward an improved metric of climate change, *Clim. Dynam.*, *20*, 843–854, doi: 10.1007/s00382-003-0305-9, 2003.
- Kaufman, Y., I. Koren, L. A. Remer, D. Rosenfeld, and Y. Rudich, Some, dust and pollution aerosol clouding the Atlantic atmosphere, submitted, 2004.
- Kaufman, Y. J., O. Dubovik, A. Smirnov, and B. N. Holben, Remote sensing of non-aerosol absorption in cloud free atmosphere, *Geophys. Res. Lett.*, *29*, 1857, doi:10.1029/2001GL014399, 2002.
- Kiehl, J. T., and B. P. Briegleb, The relative roles of sulfate aerosols and greenhouse gases in climate forcing, *Science*, *260*, 311–314, 1993.

- Kiehl, J. T., T. L. Schneider, P. J. Rasch, M. C. Barth, and J. Wong, Radiative forcing due to sulfate aerosols from simulations with the National Center for Atmospheric Research Community Climate Model, Version 3, *J. Geophys. Res.*, *105*(D1), 1441–1457, 2000.
- Koch, D., The transport and direct radiative forcing of carbonaceous and sulfate aerosols in the GISS GCM, *J. Geophys. Res.*, *106*(D17), 20,311–20,332, 2001.
- Koch, D., D. Jacob, I. Tegen, D. Rind, and M. Chin, Tropospheric sulfur simulation and sulfate direct radiative forcing in the Goddard Institute for Space Studies general circulation model, *J. Geophys. Res.*, *104*(D19), 23,799–23,822, 1999.
- Krivacsy, Z., A. Horvath, Z. Sarvari, D. Temesi, U. Baltensperger, U. Nyeki, E. Weingartner, S. Kleefeld, and S. G. Jennings, Role of organic and black carbon in the chemical composition of atmospheric aerosol at European background sites, *Atmos. Environ.*, *35*, 6231–6244, 2001.
- Laaksonen, A., P. Korhonen, M. Kulmala, and R. Charlson, Modification of the köhler equation to include soluble trace gases and slightly soluble substances, *J. Atmos. Sci.*, *55*, 853–862, 1998.
- Lacis, A. A., and J. E. Hansen, A parameterization for the absorption of solar radiation in the earth’s atmosphere, *J. Atmos. Sci.*, *31*, 118–133, 1974.
- Lacis, A. A., and M. I. Mishchenko, Climate forcing, climate sensitivity, and climate response: A radiative modeling perspective on atmospheric aerosols, in *Aerosol Forcing of Climate*, edited by R. J. Charlson and J. Heintzenberg, pp. 11–42, John Wiley & Sons, New York, 1995.
- Lacis, A. A., and V. Oinas, A description of the correlated k -distribution method for modeling nongray gaseous absorption, thermal emission, and multiple-scattering in vertically inhomogeneous atmospheres, *J. Geophys. Res.*, *96*(D5), 9027–9063, 1991.
- Leitch, W. R., C. M. Banic, G. A. Isaac, M. D. Couture, P. Liu, I. Gultepe, S.-M. Li, L. Kleinman, P. H. Daum, and J. I. MacPherson, Physical and chemical observations in marine stratus during the 1993 North Atlantic Regional Experiment: Factors controlling cloud droplet number concentrations, *J. Geophys. Res.*, *101*, 29,123–29,136, 1996.
- Lesins, G., P. Chýlek, and U. Lohmann, A study of internal and external mixing scenarios and its effect on aerosol optical properties and direct radiative forcing, *J. Geophys. Res.*, *107*(D10), 4049, doi:10.1029/2001JD000973, 2002.
- Lindberg, J. D., R. E. Douglass, and D. M. Garvey, Atmospheric particulate absorption and black carbon measurement, *Appl. Opt.*, *38*(12), 2369–2376, 1999.

- Liousse, C., J. E. Penner, C. Chuang, J. J. Walton, H. Eddleman, and H. Cachier, A global three-dimensional model study of carbonaceous aerosols, *J. Geophys. Res.*, *101*(D14), 19,411–19,432, 1996.
- Liu, P., W. R. Leitch, C. M. Banic, S.-M. Lik, and D. N. W. J. Megaw, Aerosol observations at Chebogue Point during the 1993 North Atlantic Regional Experiment: Relationships among cloud condensation nuclei, size distribution, and chemistry, *J. Geophys. Res.*, *101*, 28,971–28,990, 1996.
- Lohmann, U., and G. Lesins, Stronger constraints on the anthropogenic indirect aerosol effect, *Science*, *298*, 1012–1015, 2002.
- Martin, G. M., D. W. Johnson, and A. Spice, The measurement of parameterization of effective radius of droplets in warm stratocumulus clouds, *J. Atmos. Sci.*, *51*, 1823–1842, 1994.
- McNaughton, D. J., , and R. J. Vet, Eulerian model evaluation field study (EMEFS): A summary of surface network measurements and data quality, *Atmos. Environ.*, *30*, 227–238, 1996.
- Menon, S., and A. Del Genio, Evaluating the impacts of carbonaceous aerosols on clouds and climate, in *Human-Induced Climate Change: An Interdisciplinary Assessment*, edited by Schlesinger et al., Cambridge Univ. Press, in review, 2004.
- Mickley, L. J., P. Murti, D. Jacob, J. Logan, D. Koch, and D. Rind, Radiative forcing from tropospheric ozone calculated with a unified chemistry-climate model, *J. Geophys. Res.*, *104*, 30,135–30,172, 1999.
- Myhre, G., F. Stordal, K. Restad, and I. S. A. Isaksen, Estimation of the direct radiative forcing due to sulfate and soot aerosols, *Tellus*, *50B*, 463–477, 1998.
- Nakajima, T., A. Higurashi, K. Kawamoto, and J. E. Penner, A possible correlation between satellite-derived cloud and aerosol microphysical parameters, *Geophys. Res. Lett.*, *28*, 1171–1174, 2001.
- Nakicenovic, N., and R. Swart (Eds.), *Special Report on Emission Scenarios*, Cambridge Univ. Press, New York, 2000.
- Nenes, A., and J. H. Seinfeld, Parameterization of cloud droplet formation in global climate models, *J. Geophys. Res.*, *108*(D14), 4415, doi:10.1029/2002JD002911, 2003.
- Nenes, A., C. Pilinis, and S. N. Pandis, ISORROPIA: A new thermodynamics equilibrium model for multiphase multicomponent inorganic aerosols, *Aquat. Geochem.*, *4*, 23–152, 1998.

- Nenes, A., R. J. Charlson, M. C. Facchini, M. Kulmala, A. Laaksonen, and J. Seinfeld, Can chemical effects on cloud droplet number rival the first indirect effect?, *Geophys. Res. Lett.*, *29*, 1848–1851, 2002a.
- Nenes, A., W. C. Conant, and J. H. Seinfeld, Black carbon radiative effect on cloud microphysics and implications for the aerosol indirect effect: 2. Cloud microphysics, *J. Geophys. Res.*, *107*(D21), 4605, doi:10.1029/2002JD002101, 2002b.
- Nilsson, B., Meteorological influence on aerosol extinction in the 0.2-40 μ m wavelength range, *Appl. Opt.*, *18*(20), 3457–3473, 1979.
- Olivier, J. G. J., and J. J. M. Berdowski, EDGAR 3.x by RIVM/TNO, in *Global emission sources and sinks*, edited by J. Berdowski, R. Guicherit, and B. M. Heij, pp. 33–77, Swets & Zeitlinger Publishers, Lisse, 2001.
- Pawlowska, H., and J.-L. Brenguier, Microphysical properties of stratocumulus clouds during ACE-2, *Tellus*, *52B*, 868–887, 2000.
- Penner, J. E., H. Eddleman, and T. Novakov, Towards the development of a global inventory for black carbon emissions, *Atmos. Environ.*, *27A*, 1277–1295, 1993.
- Penner, J. E., T. Wigley, P. Jaumann, B. Santer, and K. Taylor, Anthropogenic sulfate aerosols and climate change: A method for calibrating forcing, in *Communicating About Climate: The Story of the Model Evaluation Consortium for Climate Assessment*, edited by W. Howe and A. Henderson-Sellers, pp. 91–111, Gordon and Breach Science Publishing, Sydney, 1997.
- Penner, J. E., C. C. Chuang, and K. Grant, Climate forcing by carbonaceous and sulfate aerosols, *Clim. Dynam.*, *14*, 839–851, 1998.
- Pincus, R., and M. B. Baker, Effect of precipitation on the albedo susceptibility of clouds in the marine boundary layer, *Nature*, *372*, 250–252, 1994.
- Prather, M. J., Numerical advection by conservation of second-order moments, *J. Geophys. Res.*, *91*(D6), 6671–6681, 1986.
- Quass, J., O. Boucher, and F. M. Bréon, Aerosol indirect effects in POLDER satellite data and the Laboratoire de Meteorologie Dynamique-Zoom (LMDZ) general circulation model, *J. Geophys. Res.*, *109*, D08205, doi:10.1029/2003JD004317, 2004.
- Ramanathan, V., P. J. Crutzen, J. T. Kiehl, and D. Rosenfeld, Aerosols, climate, and the hydrological cycle, *Science*, *294*(5549), 2119–2124, 2001.
- Ramaswamy, V. et al., Radiative forcing of climate change (Chapter 6), in *Climate Change 2001: The Scientific Basis*, pp. 349–416, Cambridge University Press, 2001.

- Rind, D., and J. Lerner, Use of on-line tracers as a diagnostic tool in general circulation model development: 1. horizontal and vertical transport in the troposphere, *J. Geophys. Res.*, *101*, 12,667–12,683, 1996.
- Rivera-Carpio, C. A., C. E. Corrigan, T. Novakov, J. E. Penner, C. F. Rogers, and J. C. Chow, Derivation of contributions of sulfate and carbonaceous aerosols to cloud condensation nuclei from mass size distributions, *J. Geophys. Res.*, *101*, 9483–9493, 1996.
- Roberts, D. L., and A. Jones, Climate sensitivity to black carbon aerosol from fossil fuel combustion, *J. Geophys. Res.*, *109*, D16202, doi:10.1029/2004JD004676, 2004.
- Roderick, M. L., and G. D. Farquhar, The cause of decreased pan evaporation over the past 50 years, *Science*, *298*, 1410–1411, 2002.
- Rosenfeld, D., Suppression of rain and snow by urban and industrial air pollution, *Science*, *287*, 1793–1796, 2000.
- Rosenfeld, D., and I. M. Lensky, Satellite-based insights into precipitation formation processes in continental and maritime convective clouds, *Bull. Am. Met. Soc.*, *79*, 2457–2476, 1998.
- Rosenzweig, C., and F. Abramopoulos, Land-surface model development for the GISS GCM, *J. Clim.*, *10*, 2040–2054, 1997.
- Sato, M., J. Hansen, D. Koch, A. Lacis, R. Ruedy, O. Dubovik, B. Holben, M. . Chin, and T. Novakov, Global atmospheric black carbon inferred from AERONET, *Proc. Natl. Acad. Sci.*, *100*, 6319–6324, 2003.
- Saxena, P., L. M. Hildemann, P. H. McMurry, and J. H. Seinfeld, Organics alter hygroscopic behavior of atmospheric particles, *J. Geophys. Res.*, *100*, 18,755–18,770, 1995.
- Schaap, M., H. van der Gon, F. J. Dentener, A. Visschedijk, M. van Loon, H. M. ten Brink, J. P. Putaud, B. Guillaume, C. Liousse, and P. Builtjes, Anthropogenic black carbon and fine aerosol distribution over Europe, *J. Geophys. Res.*, *109*, D18207, doi:10.1029/2003JD004330, 2004.
- Schmidt, G., R. Ruedy, J. E. Hansen, I. Aleinov, N. Bell, M. Bauer, S. Bauer, B. Cairns, Y. Cheng, A. Del Genio, G. Faluvegi, A. D. Friend, T. M. Hall, Y. Hu, M. Kelley, N. Kiang, D. Koch, A. A. Lacis, J. Lerner, K. K. Lo, R. L. Miller, L. Nazarenko, V. Oinas, J. Perlwitz, J. Perlwitz, D. T. Shindell, P. H. Stone, S. Sun, N. Tausnev, D. Thresher, and M.-S. Yao, Present day atmospheric simulations using GISS ModelE: Comparison to in-situ, satellite and reanalysis data, *J. Clim.*, submitted, 2005.

- Schwartz, S. E., Harshvardhan, and C. M. Benkovitz, Influence of anthropogenic aerosol on cloud optical depth and albedo shown by satellite measurements and chemical transport modeling, *Proceed. Nat. Acad. Sci.*, *99*, 1784–1789, 2002.
- Shine, K. P., and P. Forster, The effect of human activity on radiative forcing of climate change: a review of recent developments, *Global and Planetary Change*, *20*, 205–225, 1999.
- Shulman, M. L., M. C. Jacobson, R. J. Charlson, R. E. Synovec, and T. E. Young, Dissolution behaviour and surface tension effects of organic compounds in nucleating cloud droplets, *Geophys. Res. Lett.*, *23*, 277–280, 1996.
- Spivakovsky, C. M., J. A. Logan, S. A. Montzka, Y. J. Balkanski, M. Foreman-Fowler, D. Jones, L. W. Horowitz, A. C. Fusco, C. Brenninkmeijer, M. J. Prather, S. C. Wofsy, and M. B. McElroy, Three-dimensional climatological distribution of tropospheric OH: Update and evaluation, *J. Geophys. Res.*, *105*(D7), 8931–8980, 2000.
- Stier, P., J. Feichter, S. Kinne, S. Kloster, E. Vignati, J. Wilson, L. Ganzeveld, I. Tegen, M. Werner, Y. Balkanski, M. Schulz, and O. Boucher, The aerosol-climate model ECHAM5-HAM, *Atmos. Chem. Phys. (Discuss.)*, 2004.
- Streets, D. G., S. Gupta, S. T. Waldhoff, M. Q. Wang, T. C. Bond, and Y. Y. Bo, Black carbon emissions in China, *Atmos. Environ.*, *35*, 4281–4296, 2001.
- Taylor, K. E., and J. E. Penner, Response of the climate system to atmospheric aerosols and greenhouse gases, *Nature*, *369*, 734–737, 1994.
- Tegen, I., D. Koch, A. A. Lacis, and M. Sato, Trends in tropospheric aerosol loads and corresponding impact on direct radiative forcing between 1950 and 1990: A model study, *J. Geophys. Res.*, *105*(D22), 26,971–26,989, 2000.
- Toon, O. B., J. B. Pollack, and B. N. Khare, The optical constants of several atmospheric aerosol species: Ammonium sulfate, aluminum oxide, and sodium chloride, *J. Geophys. Res.*, *81*, 5733–5748, 1976.
- Turpin, B. J., P. Saxena, and E. Andrews, Measuring and simulating particulate organics in the atmosphere: Problems and prospects, *Atmos. Environ.*, *34*, 2983–3031, 2000.
- Twomey, S., The nuclei of natural cloud formation part II: The supersaturation in natural clouds and the variation of cloud droplet concentration, *Geophys. Pura. Appl.*, *43*, 243–249, 1959.
- Twomey, S. A., The influence of pollution on the shortwave albedo of clouds, *J. Atmos. Sci.*, *34*(7), 1149–1152, 1977.

- Twomey, S. A., M. Piepgrass., and T. L. Wolfe, An assessment of the impact of pollution on global cloud albedo, *Tellus*, *36B*, 356–366, 1984.
- United Nations Framework Convention of Climate Change (UNFCCC), *Guide to the Climate Change Negotiations Process*, available: www.unfccc.int/resource/process, 2001.
- United States Environmental Protection Agency, *Compilation of Air Pollutant Emission Factors, Volume I, AP-42*, Research Triangle Park, North Carolina, Section 13, 1991.
- United States Environmental Protection Agency, *SPECIATE version 3.1 model*, Research Triangle Park, North Carolina, available: www.epa.gov/ttn/chief/software/speciate/index.html, 1999.
- Wang, Y., J. A. Logan, and D. J. Jacob, Global simulation of tropospheric O₃-NO_x-hydrocarbon chemistry: 2. model evaluation and global ozone budget, *J. Geophys. Res.*, *103*, 10,727–10,755, 1998.
- Wesely, M. L., Parameterization of surface resistances to gaseous dry deposition in region-scale numerical models, *Atmos. Environ.*, *23*, 1293–1304, 1989.
- Wesely, M. L., and B. B. Hicks, Some factors that affect the deposition rates of sulfur dioxide and similar gases in vegetation, *J. Air Pollut. Contr. Assoc.*, *27*, 1110–1116, 1977.
- Zielinska, B. *et al.*, Northern front range air quality study final report- volume b: Source measurements, prepared for colorado state university by desert research institute, 1998.